a few amino acid substitutions (K2212M for 2/10 cases, L2232P for 1/10 cases, and L2253S for 6/10 cases) (see Fig. S2E in the supplemental material). Interestingly, the codon for amino acid 2224 encodes valine, but it was found to be variant for alanine and valine in sequences from the original patient serum (HCR6). Tupaias infected with patient serum also exhibited variability at position 2224; valine occupancy was rare, as was seen in the original HCR6 population (see Fig. S2B and C in the supplemental material). On the other hand, this position was occupied solely by valine for sequences recovered from Tup.8 (see Fig. S2E in the supplemental material), indicating that genetic variations shown for Tup.8 originated from the pHCR6 cDNA sequence. Taken together, quasispecies detection of circulating virus represents further evidence demonstrating intrinsic replication of HCV in tupaias despite low levels and infrequent detection of viremia.

DISCUSSION

In the present study, we described persistent HCV infection in tupaias. Long-term follow-up was performed and revealed histological progression of HCV-related liver disorders in infected tupaias, including steatosis, fibrosis, and cirrhosis, in addition to acute and chronic hepatitis. HCV genomic RNA was detected in animal sera intermittently throughout the entire course of infection. However, HCV RNA was detected in the liver upon sacrifice (3 years postinoculation). Furthermore, HCV RNA in serum contained genomic variants that had diverged from the inoculated virus (see Fig. S1 and S2 in the supplemental material). These data strongly indicate an established persistent infection in the tupaias studied. All animals exhibited HCV viremia soon after inoculation, yet the viremia was intermittent and accompanied by relatively low RTD-PCR titers compared with equivalent human and chimpanzee infections. The discrepancy between humans and tupaias might be due to host-dependent differences in replication efficiency. Over the course of HCV infection in these tupaias, serum ALT profiles indicated repeated liver injury, probably due to host immune responses mediated by agents such as cytotoxic T lymphocytes rather than direct viral cytopathic effects.

In cases of tupaia infection, experimental inoculations rarely led to sustained viremia, which for most human cases lasts for the entire course of infection. Even the course of infection appeared transient and self-resolved. It seems likely that HCV replication is less compatible with the tupaia host environment. This possibility was substantiated by a previous report by Xu et al. (34), where tissue-cultured virions of cloned genotype 1b, referred to as HCVcc in the paper, could not cause chronic infection with sustained viremia in tupaias. Although HCVcc actually infected most of the inoculated tupaias (83%; 10/12), chronic infection was seen for only a fraction of them (20%; 2/10). In this study, we also tried to detect a humoral response to HCV core antigen. We found that tupaia sera were HCV positive for antibodies only at occasional time points, observable as intermittent steep responses (data not shown). Overall, sustained seroconversion was not seen in this study, probably because HCV propagation in vivo was so limited or well controlled by host immunity. Given that models of HCV propagation are severely limited, the most important and interesting finding of this study is the successful detection of HCV RNA in livers of infected tupaias 3 years after inoculation, indicating that HCV persists in tupaias. Although the limited propagation of HCV in tupaias is a drawback of this model at the present time, the isolation of tupaia-adapted HCV may be feasible by performing multiple infection passages. This possibility is supported by both quasispecies development and successful reinfection.

The chimpanzee is the animal species most closely related to humans, and as a model, it has contributed significantly to our understanding of HCV infection and pathogenesis. However, reproducing HCV pathogenesis in humans or chimpanzees can take as long as 10 to 20 years. The chronically infected tupaias in the present study developed complicated liver disorders in a much shorter time. Using tupaias, with their relatively short life span (3 to 5 years in the laboratory), as a model of HCV infection, we can evaluate HCV pathogenesis and correlate senescence and duration of infection.

The recent development of a primary human hepatocyte xenograft-uPA/SCID mouse model opened up opportunities to test putative antivirals against HCV replication in vivo (10, 17). In this innovative model, human hepatocytes, which are transplanted into the lobe of a mouse liver, can support HCV replication effectively. As a result, the level of circulating HCV RNA is comparable to that of a human patient. However, this mouse model is immunodeficient, and thus, it lacks the interplay between host immunity and viral infection. Therefore, it does not provide a suitable platform for characterizing immune responses to HCV infection.

HCV infection in tupaias represents an important model of HCV infection, particularly for the study of key determinants controlling virus propagation in vivo. The pathogenesis of HCV infection can be substantially different among humans, chimpanzees, and tupaias, and the mechanisms governing these differences are of great interest. Comparative studies of HCV infection in these different species will help us to understand the basic mechanisms of persistent infection.

ACKNOWLEDGMENTS

We thank Masahiro Shuda for helpful assistance and Etsuko Endo for creating the figures. We also thank the staffs of the Departments of Microbiology and Cell Biology and Mitsugu Takahashi for breeding the tupaias.

This study was supported by grants from the Ministry of Education, Culture, Sports, Science and Technology of Japan; the Program for Promotion of Fundamental Studies in Health Sciences of the Pharmaceuticals and Medical Devices Agency of Japan; and the Ministry of Health, Labor and Welfare of Japan.

REFERENCES

1. **Abe, K., T. Kurata, Y. Teramoto, J. Shiga, and T. Shikata.** 1993. Lack of susceptibility of various primates and woodchucks to hepatitis C virus. J. Med. Primatol. **22**:433–434.
2. **Aoki, Y., H. Aizaki, T. Shimoike, H. Tani, K. Ishii, I. Saito, Y. Matsuura, and T. Miyamura.** 1998. A human liver cell line exhibits efficient translation of HCV RNAs produced by a recombinant adenovirus expressing T7 RNA polymerase. Virology **250**:140–150.
3. **Chomczynski, P., and N. Sacchi.** 1987. Single-step method of RNA isolation by acid guanidinium thiocyanate-phenol-chloroform extraction. Anal. Biochem. **162**:156–159.
4. **Choo, Q. L., G. Kuo, A. J. Weiner, L. R. Overby, D. W. Bradley, and M. Houghton.** 1989. Isolation of a cDNA clone derived from a blood-borne non-A, non-B viral hepatitis genome. Science **244**:359–362.
5. **Dash, S., G. Kalkeri, H. M. McClure, R. F. Garry, S. Clejan, S. N. Thung, and K. K. Murthy.** 2001. Transmission of HCV to a chimpanzee using virus

particles produced in an RNA-transfected HepG2 cell culture. J. Med. Virol. **65**:276–281.
6. **Flugge, P., E. Fuchs, E. Gunther, and L. Walter.** 2002. MHC class I genes of the tree shrew Tupaia belangeri. Immunogenetics **53**:984–988.
7. **Goldsmith, E. I.** 1978. The convention on international trade in endangered species of wild fauna and flora. J. Med. Primatol. **7**:122–124.
8. **Hong, Z., M. Beaudet-Miller, R. E. Lanford, B. Guerra, J. Wright-Minogue, A. Skelton, B. M. Baroudy, G. R. Reyes, and J. Y. Lau.** 1999. Generation of transmissible hepatitis C virions from a molecular clone in chimpanzees. Virology **256**:36–44.
9. **Hoofnagle, J. H.** 2002. Course and outcome of hepatitis C. Hepatology **36**:S21–S29.
10. **Inoue, K., T. Umehara, U. T. Ruegg, F. Yasui, T. Watanabe, H. Yasuda, J. M. Dumont, P. Scalfaro, M. Yoshiba, and M. Kohara.** 2007. Evaluation of a cyclophilin inhibitor in hepatitis C virus-infected chimeric mice in vivo. Hepatology **45**:921–928.
11. **Ishak, K., A. Baptista, L. Bianchi, F. Callea, J. De Groote, F. Gudat, H. Denk, V. Desmet, G. Korb, R. N. MacSween, et al.** 1995. Histological grading and staging of chronic hepatitis. J. Hepatol. **22**:696–699.
12. **Ito, T., K. Yasui, J. Mukaigawa, A. Katsume, M. Kohara, and K. Mitamura.** 2001. Acquisition of susceptibility to hepatitis C virus replication in HepG2 cells by fusion with primary human hepatocytes: establishment of a quantitative assay for hepatitis C virus infectivity in a cell culture system. Hepatology **34**:566–572.
13. **Kock, J., M. Nassal, S. MacNelly, T. F. Baumert, H. E. Blum, and F. von Weizsacker.** 2001. Efficient infection of primary tupaia hepatocytes with purified human and woolly monkey hepatitis B virus. J. Virol. **75**:5084–5089.
14. **Kolykhalov, A. A., E. V. Agapov, K. J. Blight, K. Mihalik, S. M. Feinstone, and C. M. Rice.** 1997. Transmission of hepatitis C by intrahepatic inoculation with transcribed RNA. Science **277**:570–574.
15. **Major, M. E., and S. M. Feinstone.** 1997. The molecular virology of hepatitis C. Hepatology **25**:1527–1538.
16. **Marcellin, P., T. Asselah, and N. Boyer.** 2002. Fibrosis and disease progression in hepatitis C. Hepatology **36**:S47–S56.
17. **Mercer, D. F., D. E. Schiller, J. F. Elliott, D. N. Douglas, C. Hao, A. Rinfret, W. R. Addison, K. P. Fischer, T. A. Churchill, J. R. Lakey, D. L. Tyrrell, and N. M. Kneteman.** 2001. Hepatitis C virus replication in mice with chimeric human livers. Nat. Med. **7**:927–933.
18. **Nascimbeni, M., E. Mizukoshi, M. Bosmann, M. E. Major, K. Mihalik, C. M. Rice, S. M. Feinstone, and B. Rehermann.** 2003. Kinetics of CD4+ and CD8+ memory T-cell responses during hepatitis C virus rechallenge of previously recovered chimpanzees. J. Virol. **77**:4781–4793.
19. **Pawlotsky, J. M.** 2002. Use and interpretation of virological tests for hepatitis C. Hepatology **36**:S65–S73.
20. **Ren, S., and M. Nassal.** 2001. Hepatitis B virus (HBV) virion and covalently closed circular DNA formation in primary tupaia hepatocytes and human hepatoma cell lines upon HBV genome transduction with replication-defective adenovirus vectors. J. Virol. **75**:1104–1116.
21. **Seeff, L. B.** 2002. Natural history of chronic hepatitis C. Hepatology **36**:S35–S46.
22. **Shimayama, T., S. Nishikawa, and K. Taira.** 1995. Generality of the NUX rule: kinetic analysis of the results of systematic mutations in the trinucleotide at the cleavage site of hammerhead ribozymes. Biochemistry **34**:3649–3654.
23. **Shimizu, Y. K., H. Igarashi, T. Kanematu, K. Fujiwara, D. C. Wong, R. H. Purcell, and H. Yoshikura.** 1997. Sequence analysis of the hepatitis C virus genome recovered from serum, liver, and peripheral blood mononuclear cells of infected chimpanzees. J. Virol. **71**:5769–5773.
24. **Shimizu, Y. K., A. Iwamoto, M. Hijikata, R. H. Purcell, and H. Yoshikura.** 1992. Evidence for in vitro replication of hepatitis C virus genome in a human T-cell line. Proc. Natl. Acad. Sci. USA **89**:5477–5481.
25. **Suh, Y. A., P. K. Kumar, K. Taira, and S. Nishikawa.** 1993. Self-cleavage activity of the genomic HDV ribozyme in the presence of various divalent metal ions. Nucleic Acids Res. **21**:3277–3280.
26. **Takeuchi, T., A. Katsume, T. Tanaka, A. Abe, K. Inoue, K. Tsukiyama-Kohara, R. Kawaguchi, S. Tanaka, and M. Kohara.** 1999. Real-time detection system for quantification of hepatitis C virus genome. Gastroenterology **116**:636–642.
27. **Tanaka, T., N. Kato, M. J. Cho, K. Sugiyama, and K. Shimotohno.** 1996. Structure of the 3′ terminus of the hepatitis C virus genome. J. Virol. **70**:3307–3312.
28. **Thomson, M., M. Nascimbeni, M. B. Havert, M. Major, S. Gonzales, H. Alter, S. M. Feinstone, K. K. Murthy, B. Rehermann, and T. J. Liang.** 2003. The clearance of hepatitis C virus infection in chimpanzees may not necessarily correlate with the appearance of acquired immunity. J. Virol. **77**:862–870.
29. **Tsukiyama-Kohara, K., N. Iizuka, M. Kohara, and A. Nomoto.** 1992. Internal ribosome entry site within hepatitis C virus RNA. J. Virol. **66**:1476–1483.
30. **Tsukiyama-Kohara, K., S. Tone, I. Maruyama, K. Inoue, A. Katsume, H. Nuriya, H. Ohmori, J. Ohkawa, K. Taira, Y. Hoshikawa, F. Shibasaki, M. Reth, Y. Minatogawa, and M. Kohara.** 2004. Activation of the CKI-CDK-Rb-E2F pathway in full genome hepatitis C virus-expressing cells. J. Biol. Chem. **279**:14531–14541.
31. **Walter, E., R. Keist, B. Niederost, I. Pult, and H. E. Blum.** 1996. Hepatitis B virus infection of tupaia hepatocytes in vitro and in vivo. Hepatology **24**:1–5.
32. **Wasley, A., and M. J. Alter.** 2000. Epidemiology of hepatitis C: geographic differences and temporal trends. Semin. Liver Dis. **20**:1–16.
33. **Xie, Z. C., J. I. Riezu-Boj, J. J. Lasarte, J. Guillen, J. H. Su, M. P. Civeira, and J. Prieto.** 1998. Transmission of hepatitis C virus infection to tree shrews. Virology **244**:513–520.
34. **Xu, X., H. Chen, X. Cao, and K. Ben.** 2007. Efficient infection of tree shrew (Tupaia belangeri) with hepatitis C virus grown in cell culture or from patient plasma. J. Gen. Virol. **88**:2504–2512.
35. **Yanagi, M., R. H. Purcell, S. U. Emerson, and J. Bukh.** 1997. Transcripts from a single full-length cDNA clone of hepatitis C virus are infectious when directly transfected into the liver of a chimpanzee. Proc. Natl. Acad. Sci. USA **94**:8738–8743.
36. **Yanagi, M., M. St Claire, M. Shapiro, S. U. Emerson, R. H. Purcell, and J. Bukh.** 1998. Transcripts of a chimeric cDNA clone of hepatitis C virus genotype 1b are infectious in vivo. Virology **244**:161–172.
37. **Zhao, X., Z. Y. Tang, B. Klumpp, G. Wolff-Vorbeck, H. Barth, S. Levy, F. von Weizsacker, H. E. Blum, and T. F. Baumert.** 2002. Primary hepatocytes of Tupaia belangeri as a potential model for hepatitis C virus infection. J. Clin. Invest. **109**:221–232.

THE JOURNAL OF BIOLOGICAL CHEMISTRY VOL. 284, NO. 52, pp. 36442–36452, December 25, 2009

Hepatitis C Virus Impairs p53 via Persistent Overexpression of 3β-Hydroxysterol Δ24-Reductase*[S]

Received for publication, July 10, 2009, and in revised form, October 24, 2009 Published, JBC Papers in Press, October 27, 2009, DOI 10.1074/jbc.M109.043232

Tomohiro Nishimura[‡§1], Michinori Kohara[¶1], Kosuke Izumi[‖], Yuri Kasama[‡], Yuichi Hirata[¶], Ying Huang[‖2], Masahiro Shuda[¶3], Chise Mukaidani[**], Takashi Takano[¶], Yuko Tokunaga[‡], Hideko Nuriya[¶], Masaaki Satoh[‡], Makoto Saito[‡], Chieko Kai[‖], and Kyoko Tsukiyama-Kohara[‡4]

*From the [‡]Department of Experimental Phylaxiology, Faculty of Medical and Pharmaceutical Sciences, Kumamoto University, 1-1-1 Honjo, Kumamoto, Kumamoto 860-8556, the [§]Chemo-Sero-Therapeutic Research Institute, Kikuchi Research Center, Kyokushi, Kikuchi, Kumamoto 869-1298, the [¶]Department of Microbiology and Cell Biology, Tokyo Metropolitan Institute of Medical Science, 1-6 Kamikitazawa 2-chome, Setagaya-ku, Tokyo 156-8506, the [‖]Laboratory Animal Research Center, Institute of Medical Science, University of Tokyo, 4-6-1 Shirokane-dai, Minato-ku, Tokyo 108-8639, and the **Study Service Department, PhoenixBio Company, Ltd., 3-4-1 Kagamiyama, Higashi-Hiroshima 739-0046, Japan*

Persistent infection with hepatitis C virus (HCV) induces tumorigenicity in hepatocytes. To gain insight into the mechanisms underlying this process, we generated monoclonal antibodies on a genome-wide scale against an HCV-expressing human hepatoblastoma-derived cell line, RzM6-LC, showing augmented tumorigenicity. We identified 3β-hydroxysterol Δ24-reductase (DHCR24) from this screen and showed that its expression reflected tumorigenicity. HCV induced the DHCR24 overexpression in human hepatocytes. Ectopic or HCV-induced DHCR24 overexpression resulted in resistance to oxidative stress-induced apoptosis and suppressed p53 activity. DHCR24 overexpression in these cells paralleled the increased interaction between p53 and MDM2 (also known as HDM2), a p53-specific E3 ubiquitin ligase, in the cytoplasm. Persistent DHCR24 overexpression did not alter the phosphorylation status of p53 but resulted in decreased acetylation of p53 at lysine residues 373 and 382 in the nucleus after treatment with hydrogen peroxide. Taken together, these results suggest that DHCR24 is elevated in response to HCV infection and inhibits the p53 stress response by stimulating the accumulation of the MDM2-p53 complex in the cytoplasm and by inhibiting the acetylation of p53 in the nucleus.

Hepatitis C virus (HCV)[5] is composed of a single-stranded RNA genome of positive polarity (1). Translation of viral proteins is initiated from an internal ribosome entry site (2) and results in a single polypeptide that is subsequently cleaved by host and viral proteases to yield viable proteins (3). The HCV genome does not rely on canonical translation factors and can readily establish chronic infection without integrating into the host genome, resulting in hepatic steatosis and hepatocellular carcinoma (HCC) (4). More than 170 million people worldwide are infected with HCV (5); chronic HCV infection and aging are the major risk factors for HCC (6–8). Liver cancer is the fifth most common cause of cancer mortality worldwide (9). The frequent inactivation of p53 in human HCC suggests that the loss of p53-dependent apoptosis may promote hepatocarcinogenesis (10). Chronic HCV infection results in chronic liver inflammation and induces endoplasmic reticulum stress and oxidative stress, which are thought to induce hepatocarcinogenesis (11, 12). The mechanistic details underlying HCC development are not fully understood. To gain insight into the molecular mechanisms underlying HCV-induced pathogenesis, we previously established RzM6 cells (13), a human hepatoblastoma (HepG2)-derived cell line in which expression of the full-length HCV genome is controlled by a Cre/*loxP* system. Expression of the HCV genome promoted anchorage-independent growth of RzM6 cells after 44 days of culture from the onset of HCV expression (RzM6-44d cells) but not in RzM6 cells after 0 days (RzM6-0d cells) (13). In the present study, we generated monoclonal antibodies against RzM6 cells cultured for longer than 44 days (RzM6-LC cells) and then screened the antibodies for their ability to bind antigens overexpressed in these cells. We identified 3β-hydroxysterol Δ24-reductase (DHCR24) from this screen and characterized its role in the HCV-induced cell growth deregulation.

EXPERIMENTAL PROCEDURES

Cells, Growth Assay, and Plasmids—HepG2 human hepatoblastoma cells, HuH-7 human hepatoma cells, WRL68 human embryonic hepatic cells, HEK293 human embryonic kidney cells, and human WI38 fibroblast cells were purchased from the American Type Culture Collection. NIH3T3 mouse fibroplast cells were from Japanese Collection of Research Bioresource. Cells were cultured under the growth conditions described in the supplemental material. RzM6 cells were established by

* This work was supported by grants from the Ministry of Health and Welfare of Japan, the Ministry of Education, Culture, Sports, Science and Technology of Japan, the Program for Promotion of Fundamental Studies in Health Sciences of the National Institute of Biomedical Innovation, the Cooperative Research Project on Clinical and Epidemiological Studies of Emerging and Re-emerging Infectious Diseases, and the Hayashi Memorial Foundation for Female Natural Scientists.

[S] The on-line version of this article (available at http://www.jbc.org) contains supplemental Figs. 1–5.

[1] Both authors contributed equally to this work.

[2] Present address: Liver Diseases Branch, NIDDK, National Institutes of Health, Bethesda, MD 20892.

[3] Present address: Molecular Virology Program, University of Pittsburgh Cancer Institute, University of Pittsburgh, 5117 Centre Ave., Pittsburgh, PA 15213.

[4] To whom correspondence should be addressed. Tel.: 81-96-373-5560; Fax: 81-96-373-5560; E-mail: kkohara@kumamoto-u.ac.jp.

[5] The abbreviations used are: HCV, hepatitis C virus; HCC, hepatocellular carcinoma; siRNA, small interfering RNA; HA, hemagglutinin; ELISA, enzyme-linked immunosorbent assay; HBV, hepatitis B virus.

transfection of HepG2 cells with the plasmid *HCR6*-Rz, which contains the full-length HCV cDNA (nucleotides 1–9611; GenBank™ accession number AY045702), and stably transformed cell lines were selected in media containing G418 (800 μg/ml bioactive; Invitrogen). These cell lines, termed 2–18, were then transfected with pCAG-Mer-Cre-Mer (Cre/*loxP* system) and were selected in media containing puromycin (Sigma), as described previously (13), to generate the RzM6 cell line. HCV expression was induced by treatment with 4-hydroxy-tamoxifen (100 nM). Cells expressing HCV for 44 days (RzM6-44d cells) displayed augmented anchorage-independent cell growth. Cells expressing HCV for more than 44 days are referred to as RzM6-LC cells.

The tumor formation assay was performed by injecting RzM6-0d, RzM6-44d, or RzM6-LC cells in the exponential growth phase into nude mice. Cells in culture were harvested with trypsin, and 2×10^6 or 1×10^7 cells were subcutaneously injected into the backs of athymic nude mice (ICR strain, Charles River). HepG2 and WRL68 cells with plasmid DNA or small interfering RNA (siRNA) were transiently transfected using Lipofectamine 2000 or RNAi Max (Invitrogen). HepG2 cells transfected with the pcDNA3.1-based HA- and FLAG-tagged DHCR24 expression vector were selected in media containing 800 μg/ml G418 (Invitrogen). The terminal deoxynucleotidyltransferase-mediated dUTP nick end labeling assay was performed using the TMR red *in situ* cell death detection kit (Roche Applied Science).

Generation of Monoclonal Antibodies—BALB/c mice received seven or eight intraperitoneal injections of RzM6-44d cells (5×10^6 cells/injection) in RIBI adjuvant (trehalose dimycolate + monophosphoryl lipid A emulsion; RIBI ImmunoChemResearch) at 3–4-week intervals. At the end of this immunization regimen, the spleens were removed, and the splenocytes were fused with mouse myeloma PAI cells using polyethylene glycol 1500 (Roche Applied Science), as described previously (14). Hybridoma cells were selected in medium containing hypoxanthine, aminopterin, and thymidine (Invitrogen), and culture supernatants were collected for whole-cell enzyme-linked immunosorbent assay (ELISA) screening.

ELISA, Immunostaining, Northern Blotting, Western Blotting, and Immunoprecipitation—Immunofluorescence assays, whole-cell ELISA, standard ELISA, and immunostaining are described in the supplemental materials. Northern blotting was performed as described previously (13). For immunoprecipitation and Western blotting, frozen specimens were homogenized on ice using a Dounce homogenizer fitted with a type-A pestle (Wheaton Science Products) in radioimmune precipitation buffer (1% SDS, 0.5% (v/v) Nonidet P-40, 0.15 M NaCl, 10 mM Tris, pH 7.4, 5 mM EDTA, and 1 mM dithiothreitol). Western blotting was performed as previously described (13) with the following primary antibodies: anti-DHCR24 monoclonal antibody 2-152a, polyclonal anti-p53 (Cell Signaling Technologies), anti-MDM2 (murine double minute clone 2 oncoprotein) (Santa Cruz Biotechnology, Inc., Santa Cruz, CA), anti-Myc (9E10) (Santa Cruz Biotechnology, Inc.), and anti-HCV core protein monoclonal antibody 515 (15) or 31-2. Anti-p53 monoclonal antibody (DO-1) and polyclonal antibody (FL-393) (Santa Cruz Biotechnology, Inc.) were used for immunostaining. Phosphorylation of p53 was characterized by Western blotting with antibodies against phosphorylated Ser^6, Ser^9, Ser^{15}, Ser^{20}, Ser^{37}, Ser^{46}, and Ser^{329} (Cell Signaling Technologies). Acetylation of p53 was examined by immunoprecipitation with anti-p53 (DO-1) and the ExactaCruz immunoprecipitation reagent (Santa Cruz Biotechnology, Inc.), followed by Western blotting with antibodies against p53 (rabbit polyclonal; Cell Signaling) or acetylated p53 (Lys^{373}/Lys^{382}) (Upstate Biotechnology). The interaction between p53 and MDM2 was examined by immunoprecipitation with anti-p53 (FL-393) or anti-MDM2 (H221; Santa Cruz Biotechnology, Inc.) and protein A-Sepharose (GE Healthcare), followed by Western blotting with monoclonal antibodies against MDM2 (SMP14, Santa Cruz Biotechnology, Inc.) and p53 (DO-1), respectively. Polyclonal anti-actin (Santa Cruz Biotechnology, Inc.), anti-histone H1 (Santa Cruz Biotechnology, Inc.), and anti-heat shock protein 70 (HSP70) (Stressgen) primary antibodies were used for normalization of Western blots. Subcellular fractionation of RzM6-0d and LC cells was performed as previously described (15).

Cloning and Expression of DHCR24 and in Vitro Translation—Total RNA was isolated from 1×10^6 HuH-7 cells using ISOGEN Reagent (Nippon Gene). Purified RNA (2 μg) was reverse-transcribed with Superscript II (Invitrogen) using random primers according to the manufacturer's protocol. The DHCR24 cDNA was then amplified by PCR with Phusion DNA polymerase (BioLabs). The following primers were used for the first round of amplification: D-5-1 (5′-CCCGGGCTGTGGGCTACAGG-3′, forward) and D-3-1 (5′-CCAGGCCACTTTTATTTAAA-3′, reverse). Primers for the second round of amplification were D-5-2 (5′-GTTCTCGAGCAGTGACAGGAGGCGCGAAC-3′, forward) and D-3-2 (5′-GTTCTCGAGTCCAGGCGGGCTCCAGCTCA-3′, reverse). The amplified DHCR24 cDNA was subcloned into the pGEM-T easy vector (Promega). *In vitro* translation was performed using TNT(R) reticulocyte lysate (Promega) and the Express Protein Labeling Mix (New England Nuclear) in the presence of either [^{35}S]Met/Cys or non-radioactive methionine. Amplified DHCR24 cDNA was digested with XhoI and subcloned into the pCAG-PURO vector (16) for transfection into WRL68 cells using Lipofectamine 2000. Amplified DHCR24 cDNA was also subcloned into the pcDNA3.1 vector containing an HA or FLAG tag (kindly supplied by Dr. N. Takahashi, Tokyo University of Agriculture and Technology) for transfection into RzM6 or HepG2 cells using Lipofectamine LTX (Invitrogen). Transfected cells were selected in media containing G418.

The lentiviral vector, pCSII-EF-MCS-EMCV IRES-GFP (generous gift from Hiroyuki Miyoshi, RIKEN, Tsukuba, Japan), was modified by replacing the green fluorescent protein gene with the hygromycin phosphotransferase gene to construct pCSII-EF-MCS-EMCV IRES-Hygro. DHCR24 fused to the 5′-HA or 5′-FLAG tag-encoding sequence were cloned under the EF promoter. The resulting plasmid was cotransfected with packaging plasmid (pCAG-HIVgp and pCMV-VSVG-RSV-Rev) in 293FT cells (Invitrogen) to produce recombinant lentivirus. Following infection, cells were selected with hygromycin B (600 μg/ml; Sigma).

Silencing of DHCR24 and HCV by siRNA—The DHCR24 stealth siRNA was designed to target the human DHCR24 mRNA sequence 5′-GCAAGCUGAAUAGCAUUGGCAAUUA-3′ (nucleotides 970–993) using the BLOCK-iT RNAi designer (Invitrogen). A mutated siRNA (5′-GCAGUCUAACGAUUACGGAAAGUUA-3′) was synthesized as a control. An alternative siRNA, siDHCR24-1024, was designed as 5′-GAGAACUAUCUGAAGACAATT-3′. The HCV siRNA was synthesized as previously described (17). Cells were transfected with a 1 nM concentration of the chemically synthesized siRNAs using Lipofectamine 2000 or Lipofectamine RNAiMAX (Invitrogen) in Opti-MEM (Invitrogen) and then incubated for 4–6 h at 37 °C. Cells were characterized 48 h after transfection.

Caspase and Reporter Assays—Cells (1×10^4 cells/well) were seeded into white 96-well plates (Sumitomo Bakelite), treated with 1 mM H_2O_2, and then lysed with caspase-Glo 3/7 buffer (Promega). Caspase 3/7 activity was determined by measuring the absorbance resulting from cleavage of a proluminescent substrate containing the sequence DEVD (Promega) using a multilabel counter (PerkinElmer Life Sciences). The $p21^{WAF1/CIP1}$ promoter activity was assayed in HepG2, RzM6-0d, or RzM6-LC cells transfected with pWWP-Luc (kindly supplied by Dr. Bert Vogelstein (The Johns Hopkins University)). Cells were cotransfected with phRL-TK(Int-) (Promega) for normalization of promoter activity. Cells were incubated for 2 days after transfection and were then treated with 1 mM H_2O_2 for 4 h. Promoter activity was measured using the Dual-Luciferase reporter assay system (Promega).

HCV Infection of Humanized Chimeric Mouse Liver and mRNA Quantification by Quantitative Reverse Transcription-PCR—Detailed procedures are described in the supplemental material.

Statistical Analysis—Student's *t* test was used to test the statistical significance of the results. *p* values less than 0.05 were considered statistically significant.

RESULTS

Expression of DHCR24 Parallels Hepatocarcinogenesis—RzM6 cells expressing full-length HCV were established using the Cre/*loxP* expression-switching system (13). RzM6 cells cultured for longer than 44 days (termed RzM6-LC) had a greater ability to form colonies (13) and to induce tumors in nude mice (Fig. 1*A*). We produced monoclonal antibodies against RzM6-LC cells (see supplemental materials) and screened them for their ability to bind RzM6 antigens overexpressed upon the onset of hepatocarcinogenesis. Antibody clone 2-152a bound to a ~60-kDa protein (p60) that was expressed at higher levels in RzM6-LC cells than in RzM6 cells before the onset of HCV expression (termed RzM6-0d) (13) (Fig. 1*B*). p60 was strongly expressed in hepatoma-derived HuH-7 cells but was less abundant in the less aggressive cancer cell line, HepG2, or in the normal embryonic cell lines WRL68, HEK293, or NIH3T3 (supplemental Fig. 1*A*). To identify p60, the protein was purified from RzM6-LC cells using immunoaffinity chromatography and subjected to matrix-assisted laser desorption/ionization time-of-flight mass spectrometry (supplemental Fig. 1*B*). Through this process, p60 was identified as DHCR24 (also

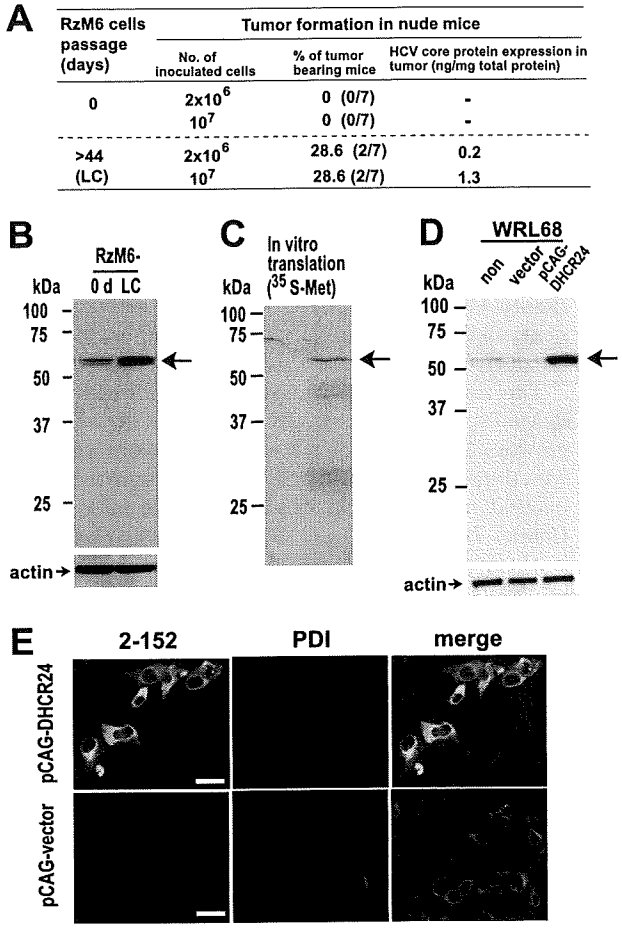

FIGURE 1. **Analysis of RzM6 cell tumorigenicity and identification of DHCR24 overexpression in RzM6-LC cells.** *A*, summary of tumor formation in nude mice injected with RzM6-0d or RzM6-LC cells. *B*, detection of a ~60-kDa protein (*arrow, upper panel*) in whole-cell lysates (30 μg/lane) from RzM6-0d and RzM6-LC cells by Western blotting with monoclonal antibody 2-152a. Anti-actin antibody was used for normalization (*arrow, lower panel*). Data are representative of two independent experiments. *C*, empty vector (pGEM3, *left lane*) or pGEM-DHCR24 (*right lane*) was subjected to *in vitro* transcription/translation using rabbit reticulocyte lysates in the presence of [^{35}S]methionine. Samples were subjected to SDS-PAGE followed by autoradiography. *D*, cell lysates from untransfected WRL68 cells (*non*), WRL68 cells transfected with empty pCAG vector (*vector*), and WRL68 cells transfected with pCAG-DHCR24 vector were examined by Western blotting with monoclonal antibody 2-152a (*upper panel*) or monoclonal anti-actin antibody (*lower panel*). *E*, WRL68 cells were transfected with pCAG-DHCR24 or pCAG vector alone and subjected to immunocytochemistry with monoclonal antibody 2-152a (*green*) or anti-protein-disulfide isomerase antibody (*PDI*; *red*). *Scale bars*, 25 nm.

known as seladin-1) (18–20), an enzyme that catalyzes the reduction of the Δ-24 double bond of sterol intermediates during cholesterol biosynthesis and is up-regulated by oxidative stress (19, 21). DHCR24 cDNA was cloned and translated *in vitro* (Fig. 1*C*) and also expressed in human embryonic hepatic WRL68 cells (Fig. 1*D*), and the monoclonal antibody 2-152a reacted with the expressed protein (Fig. 1, *D* and *E*).

HCV Induces Persistent DHCR24 Overexpression—Since DHCR24 was up-regulated in RzM6-LC cells, we examined whether HCV can induce DHCR24 expression in human hepatocytes. We also compared the expression levels of DHCR24

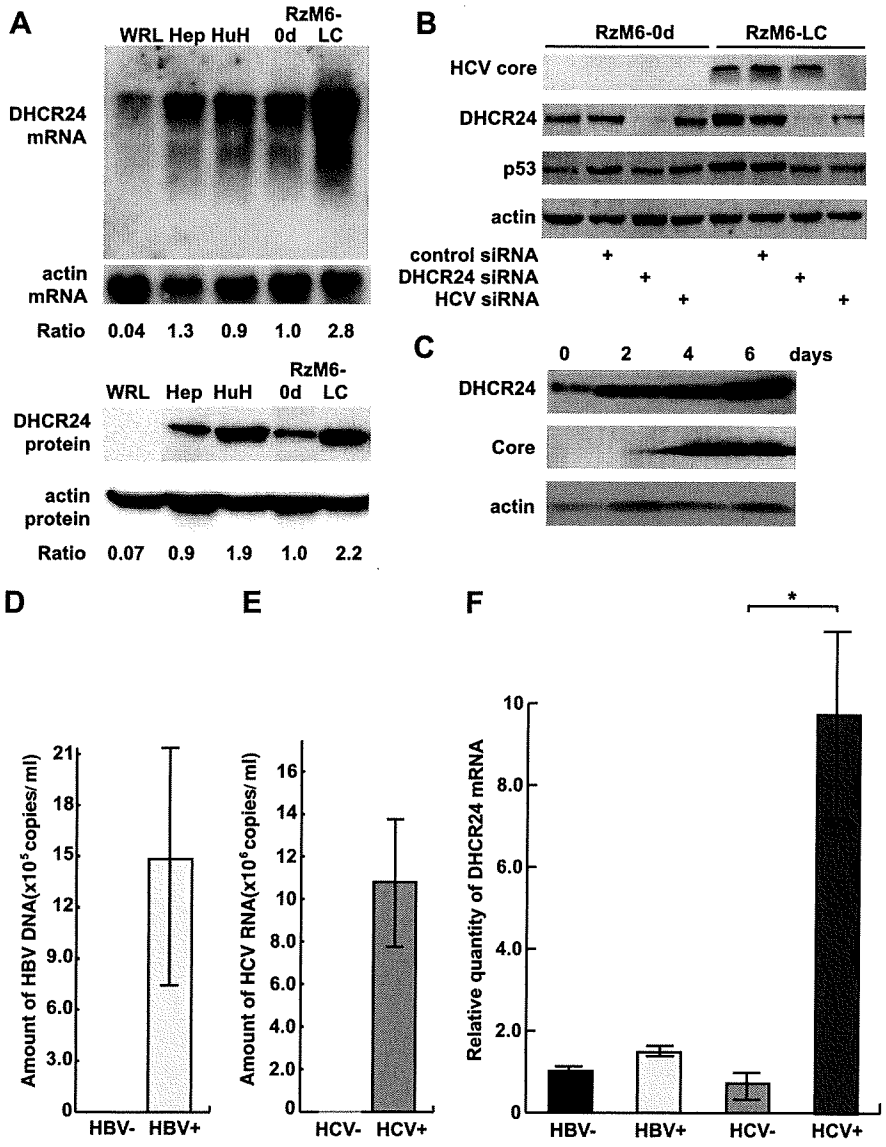

FIGURE 2. **Induction of DHCR24 by HCV in human liver cell lines.** *A*, expression of DHCR24 mRNA (Northern blot, *upper panel*) and protein (Western blot, *lower panel*) in WRL68 (*WRL*), HepG2 (*Hep*), HuH-7 (*HuH*), RzM6-0d, and RzM6-LC cells. Ratios indicate the amount of DHCR24 mRNA or protein in each cell type (quantified by densitometry) relative to that of RzM6-0d cells. *B*, Western blotting of HCV core protein, DHCR24, and p53 (DO-1 antibody) proteins in RzM6-0d and RzM6-LC cells following treatment with the indicated (+) siRNA. *C*, the induction of DHCR24 by HCV after 2, 4, and 6 days in RzM6 cells by treatment of tamoxifen (100 nM). Data are representative of two independent experiments, and anti-actin antibody was used as a loading control (*A–C*). *D*, amount of HBV DNA in HBV-infected human hepatocytes in chimeric mouse liver quantitated by RTD-PCR. *E*, amount of HCV-RNA in HCV-infected human hepatocytes in chimeric mouse liver quantitated by RTD-PCR. *F*, the quantitation of DHCR24 mRNA in mock-infected, HBV-infected, and HCV-infected human hepatocytes in chimeric mouse liver. *Vertical bars*, S.D.; *, $p < 0.05$ (two-tailed Student's *t* test).

protein and mRNA in a panel of hepatic and embryonic cell lines (Fig. 2*A*). Northern blotting revealed that DHCR24 mRNA expression was notably higher in RzM6-LC cells than in RzM6-0d cells, indicating that induction of DHCR24 occurs at the transcriptional level. DHCR24 protein levels were also higher in HuH-7 and RzM6-LC cells relative to RzM6-0d cells (Fig. 2*A*). To examine whether persistent up-regulation of *DHCR24* in RzM6-LC cells resulted from HCV expression, we utilized an siRNA to knockdown HCV expression (17) (Fig. 2*B*). Silencing HCV by greater than 99% with siRNA reduced the expression of DHCR24 and p53 in RzM6-LC cells. When we induced HCV expression with tamoxifen, the induction of DHCR24 was observed after 2, 4, and 6 days (Fig. 2*C*). These results indicate that expression of the full-length HCV genome induced DHCR24 overexpression. DHCR24 was not induced in HuH-7 cells infected with the HCV strain JFH-1 (22) (data not shown). This result might be explained by the substantial endogenous expression of DHCR24 in HuH-7 cells (Fig. 2*A* and supplemental Fig. 1*A*). To examine whether HCV infection can induce DHCR24, human hepatocytes in chimeric mice were infected with hepatitis B virus (HBV) or HCV (Fig. 2, *D* and *E*). Notable up-regulation of DHCR24 mRNA was detected in HCV-infected human hepatocytes but not in HBV-infected human hepatocytes (Fig. 2*F*).

Persistent Overexpression of DHCR24 Induces Apoptotic Resistance to Oxidative Stress—As HCV infection increased the expression of DHCR24, we further examined the effect of DHCR24 on hepatocytes. Because DHCR24 regulates oxidative stress-induced apoptosis (19, 21, 23, 24), the terminal deoxynucleotidyltransferase-mediated dUTP nick end labeling assay was performed with RzM6 cells to examine the effect of DHCR24 overexpression on H_2O_2-induced apoptosis (Fig. 3*A*). Fragmentation of genomic DNA was less pronounced in DHCR24-overexpressing cells (RzM6-LC cells and RzM6-0d cells transduced with DHCR24 lentivirus) than in RzM6-0d cells or RzM6-0d cells transduced with empty lentiviral vector. To quantify the apoptotic response, we examined the effect of DHCR24 overexpression on caspase activity (Fig. 3, *B–D*). Caspase activation by H_2O_2 was suppressed in RzM6-LC cells compared with RzM6-0d cells (Fig. 3*B*). Transfection with HCV siRNA recovered the caspase response in RzM6-LC cells. Caspase 3/7 activity was also examined following the transfection of HepG2 cells with pCA-Rz (Fig. 3*C*). Induction of caspase activation by H_2O_2 was inhibited by expression of the HCV gene; the inhibition was partially recovered by transfection with DHCR24

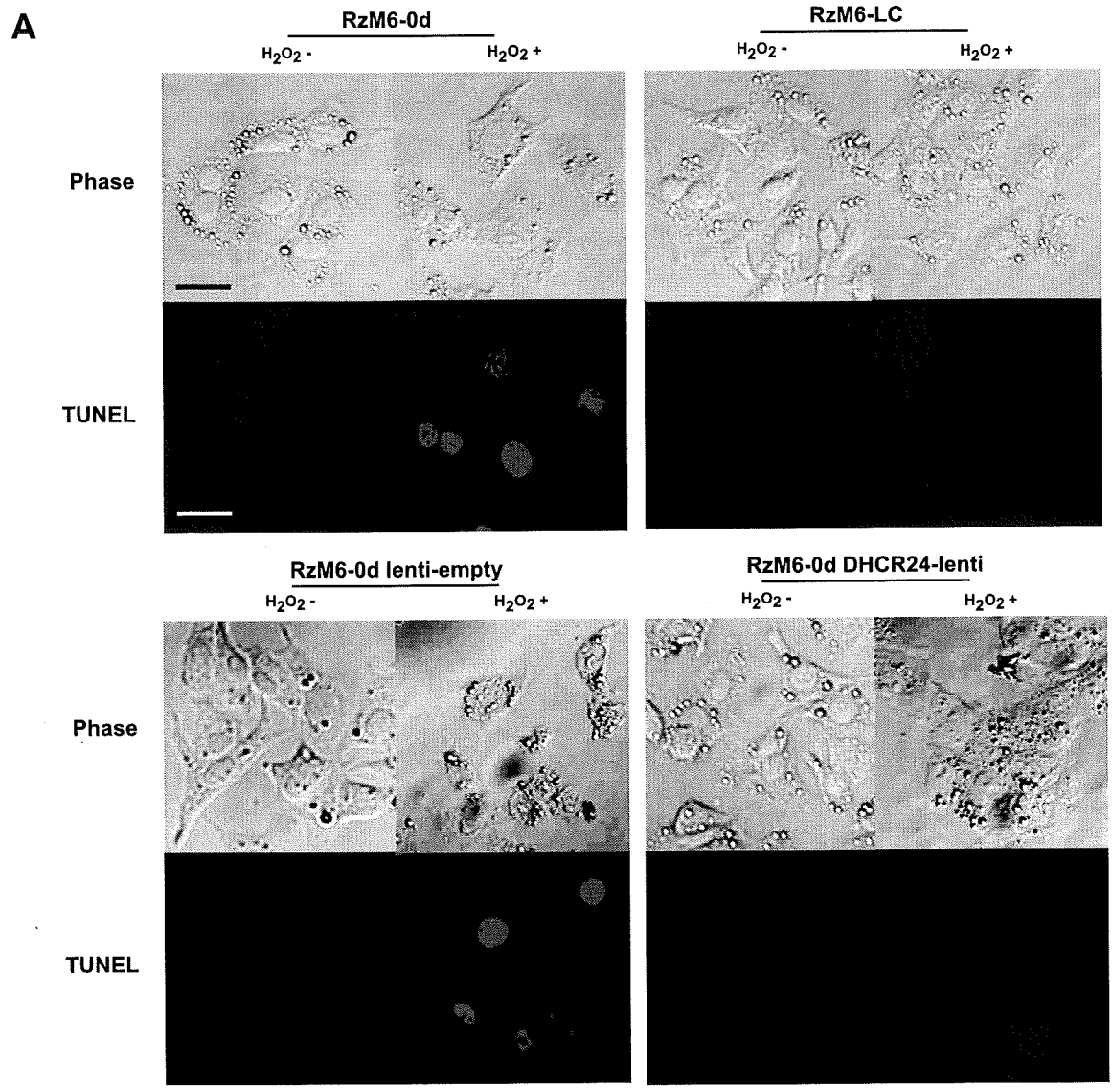

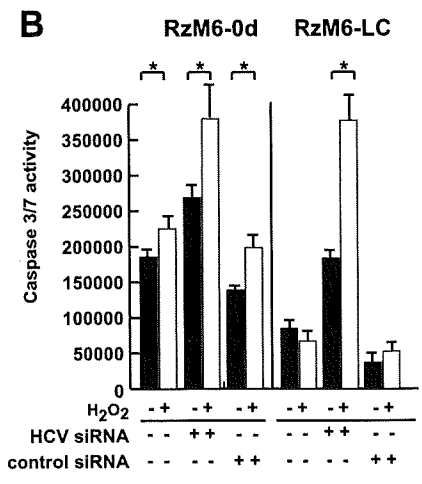

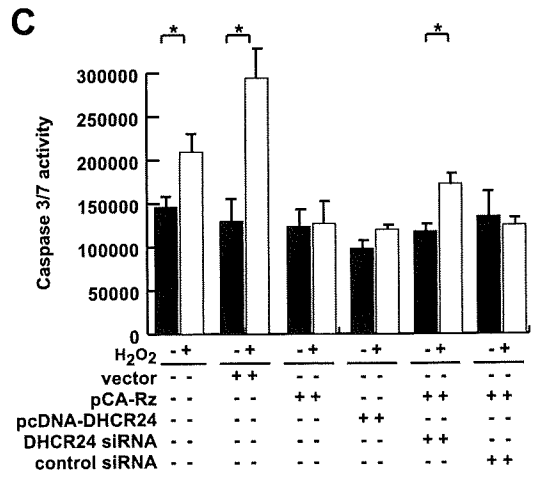

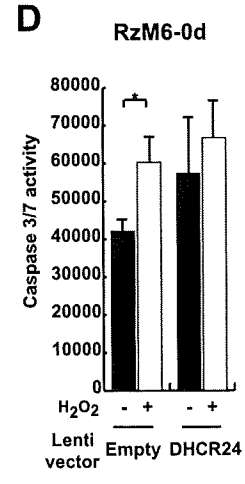

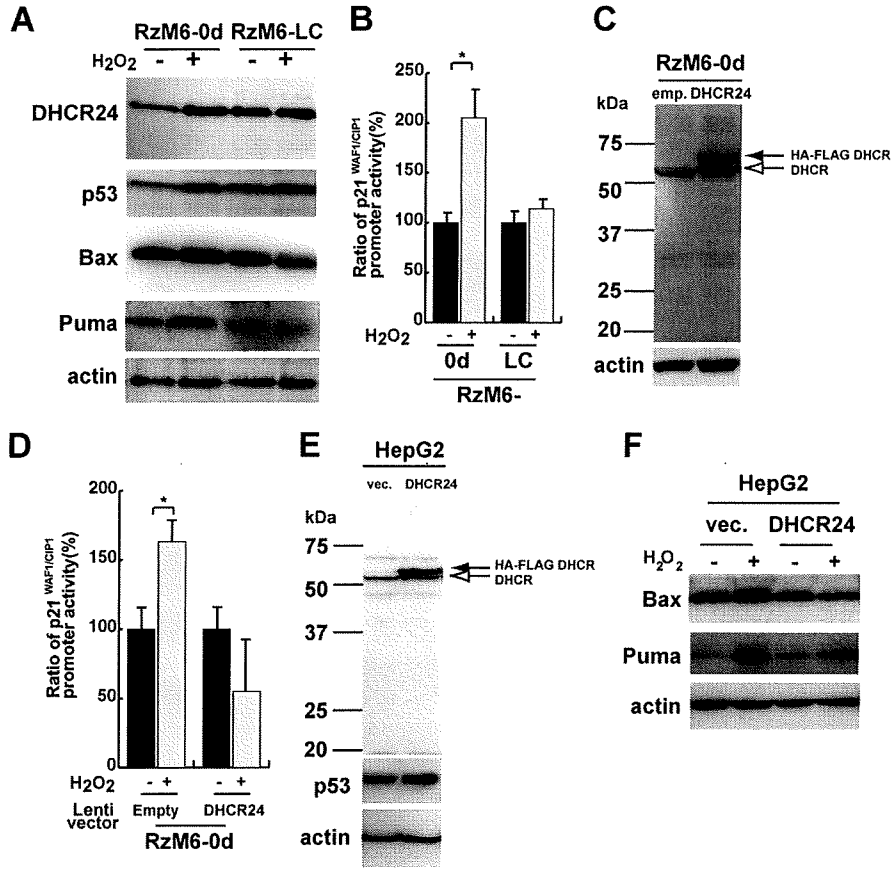

FIGURE 4. **Persistent overexpression of DHCR24 impairs p53 activity.** *A*, Western blotting of RzM6-0d and RzM6-LC cells treated with or without H_2O_2 was performed using antibodies against the proteins indicated on the *left*. *B*, $p21^{WAF1/CIP1}$ promoter activity in RzM6-0d and RzM6-LC cells transfected with pWWP-Luc followed by treatment with or without H_2O_2. Promoter activity was calculated as the ratio of firefly luciferase activity to *Renilla* luciferase activity. The ratio of promoter activity with H_2O_2 treatment to without H_2O_2 treatment is indicated as a percentage. *C*, DHCR24 expression in RzM6-0d cells transduced with lenti-empty (*emp.*) or lenti-DHCR24 (with HA-FLAG tag) vector. *D*, $p21^{WAF1/CIP1}$ promoter activity in RzM6-0d cells transfected with lenti-empty or lenti-DHCR24 vector followed by treatment with or without H_2O_2. Promoter activity was calculated as the ratio of firefly luciferase activity to *Renilla* luciferase activity. The ratio of promoter activity with H_2O_2 treatment to activity without H_2O_2 treatment is indicated as a percentage. *E*, HepG2 cells transfected with pcDNA vector (*vec*) or DHCR24 expression vector (pcDNA-DHCR24 HA-FLAG tag; *DHCR24*) and selected by G418 were analyzed by Western blotting with DHCR24 monoclonal antibody 2-152a (*top*), p53 monoclonal antibody (DO-1) (*middle*), and actin (*bottom*). *F*, expression of Bax and Puma in HepG2 cells transfected with pcDNA vector (*vec*) or pcDNA-DHCR24 vector followed by treatment with or without H_2O_2 was analyzed by Western blotting with antibodies to the proteins indicated at the *left*. Actin was analyzed as a control. In *A–F*, representative data from three independent experiments are shown; *, $p < 0.05$ (two-tailed Student's *t* test).

siRNA. Moreover, overexpression of DHCR24 from a lentivirus vector (Fig. 3*D*) (25) or from transfection with a DHCR24 expression vector (data not shown) impaired H_2O_2-induced caspase activation in RzM6-0d cells. Thus, enhanced expression of DHCR24 promotes resistance to H_2O_2-induced apoptotic responses, and HCV-induced apoptotic resistance is partially mediated by DHCR24.

Persistent Overexpression of DHCR24 Inhibits p53 Activity—H_2O_2 induces p53-dependent apoptosis (26). Expression of the p53-induced apoptotic response mediators, Bax (27) and Puma (28), did not increase after H_2O_2 treatment of RzM6-LC cells (Fig. 4*A*). Therefore, we examined p53 expression and function in DHCR24-overexpressing cells. H_2O_2 increased the expression of DHCR24 and p53 in RzM6-0d cells. By comparison, the expression of these proteins was already elevated prior to H_2O_2 treatment in RzM6-LC cells, and we found no further H_2O_2-induced increase in expression (Fig. 4*A*). Consistent with these findings, H_2O_2 activated transcription from the $p21^{WAF1/CIP}$ promoter in RzM6-0d cells but not in RzM6-LC cells (Fig. 4*B*). This response of the $p21^{WAF1/CIP}$ promoter is impaired in cells overexpressing DHCR24 via the lentivirus vector (Fig. 4, *C* and *D*) or via the expression vector (Fig. 4*E*). Induction of Bax and Puma expression after H_2O_2 treatment was decreased in DHCR24-overexpressing cells (Fig. 4*F*). These results indicate that although p53 expression is elevated in DHCR24-overexpressing cells, the function of p53 in the oxidative stress pathway is impaired.

Overexpression of DHCR24 Enhances the Interaction between p53 and MDM2—Since DHCR24 is a regulator of the p53-MDM2 interaction (21), we examined the interaction between p53 and its specific ubiquitin ligase, MDM2. Unexpectedly, the interaction between p53 and MDM2 was stronger in RzM6-LC cells than in RzM6-0d cells (Fig. 5, *A* and *B*). Lentiviral vector overexpression of DHCR24 in RzM6-0d cells increased the binding of p53 to MDM2 (data not shown). Furthermore, cell fractionation analysis revealed that the interaction between MDM2 and p53 mostly occurred in the cytoplasmic fraction, even after H_2O_2

FIGURE 3. **Prior overexpression of DHCR24 inhibits H_2O_2-induced apoptosis.** *A*, representative phase-contrast images of RzM6-0d and RzM6-LC cells (*upper panels*) or lenti-empty and lenti-DHCR24 vector-transduced RzM6-0d cells (*lower panels*) treated with or without H_2O_2 (1 mM, 4 h). *In situ* cell death was detected by the terminal deoxynucleotidyltransferase-mediated dUTP nick end labeling (*TUNEL*) assay with tetramethylrhodamine. *Scale bars*, 25 nm. Representative data from three experiments are shown. *B*, caspase 3/7 activity (relative light units) in RzM6-0d and RzM6-LC cells treated with or without H_2O_2. Cells were transfected with or without HCV siRNA or with control siRNA as indicated. *C*, caspase 3/7 activity in HepG2 cells treated with or without H_2O_2. Cells were transfected with control pcDNA vector (vector), pCA-Rz, pcDNA-DHCR24, DHCR24 siRNA, or control siRNA. *D*, caspase 3/7 activity in RzM6-0d cells treated with or without H_2O_2. Cells were transduced with lenti-empty or lenti-DHCR24 vector. In *B–D*, data reflect the means ± S.D. of three independent triplicate experiments; *, $p < 0.05$ (two-tailed Student's *t* test).

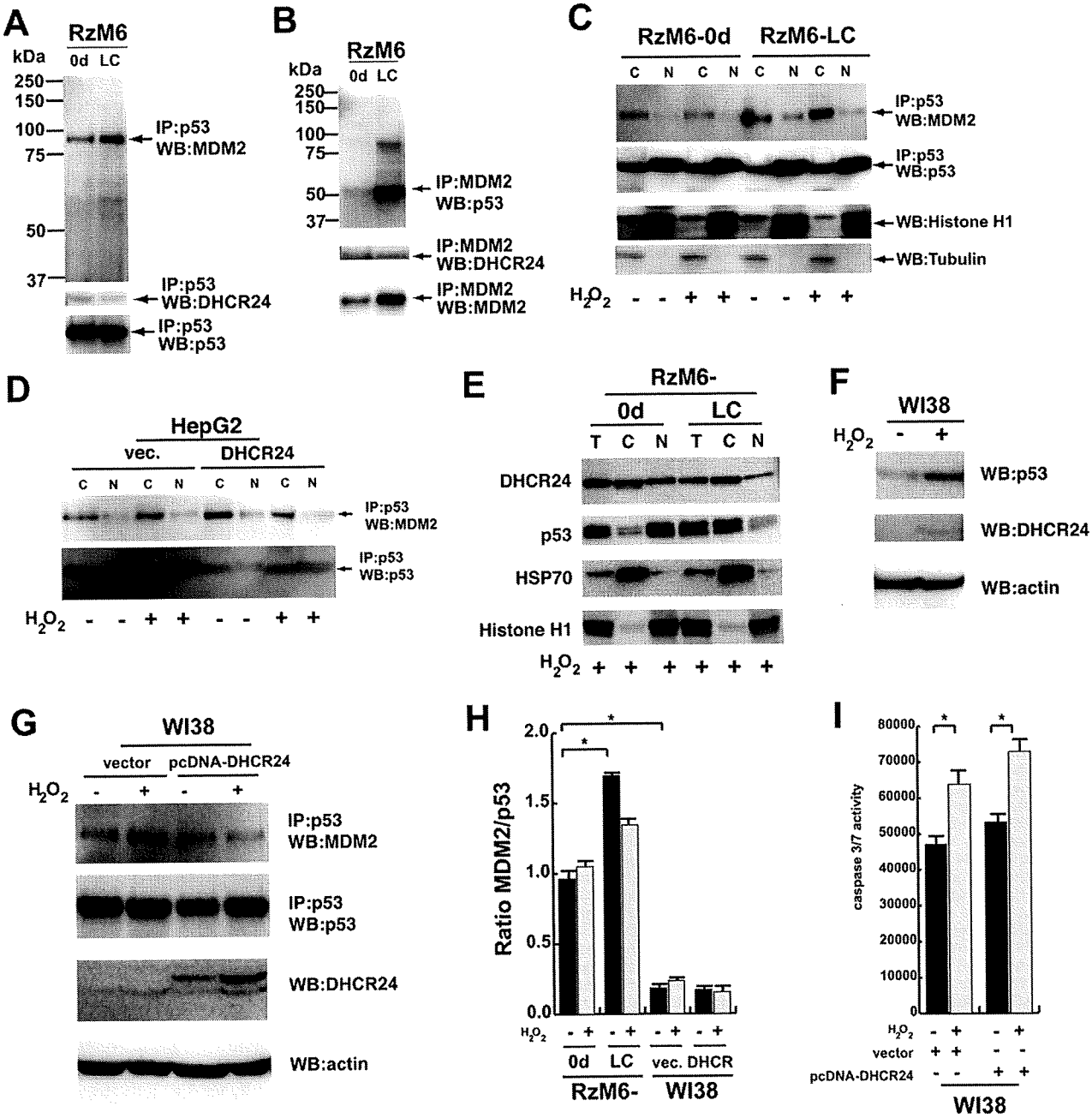

FIGURE 5. **DHCR24 overexpression enhances the interaction between p53 and MDM2 in the cytoplasm.** *A*, p53 was immunoprecipitated (*IP*) from RzM6-0d and RzM6-LC cells with polyclonal anti-p53 antibody (FL393) followed by Western blotting with monoclonal antibodies against MDM2 (*top*) and p53 or DHCR24 (*bottom*). *B*, MDM2 was immunoprecipitated from RzM6-0d and RzM6-LC cells using polyclonal anti-MDM2 antibody (H221) followed by Western blotting (*WB*) with monoclonal antibodies against p53 (*top*) and MDM2 or DHCR24 (*bottom*). *C*, p53 was immunoprecipitated from cytoplasmic (*C*) or nuclear (*N*) fractions of RzM6-0d and LC cells using anti-p53 antibody (FL393) followed by Western blotting with anti-MDM2 antibody (*top*) and anti-p53 antibody (*bottom*). Cell fractionation was confirmed by Western blotting with anti-histone H1 and tubulin (*WB*). *D*, p53 was immunoprecipitated from cytoplasmic or nuclear fractions of HepG2 cells transfected with control pcDNA (*vec*) or pcDNA-DHCR24 expression vector using polyclonal anti-p53 (FL393) followed by Western blotting with antibodies against the proteins indicated at the right. Reaction with secondary antibodies (anti-rabbit or mouse IgG conjugated with horseradish peroxidase) alone did not show any signal (data not shown), and data representative of three independent experiments are shown (*A–D* and *G*). *E*, RzM6-0d or RzM6-LC cells with H_2O_2 treatment were fractionated into total (*T*), cytoplasmic, and nuclear fractions and subjected to Western blotting with the antibodies indicated on the *left*. *F*, Western blotting of WI38 cells with or without H_2O_2 treatment (0.5 mM, 4 h) with antibodies against p53, DHCR24, and actin. *G*, immunoprecipitation of p53 from cells transfected with pcDNA vector and pcDNA-DHCR24 (*DHCR*) with or without H_2O_2 treatment (0.5 mM, 4 h), followed by Western blotting with antibodies against MDM2 (*first column*) and p53 (*second column*). Cells were examined with Western blotting with anti-DHCR24 (*third column*) and anti-actin (*fourth column*). *H*, the average ratio of the quantified results of immunoprecipitation of p53 and Western blotting of MDM2 in RzM6-0d, RzM6-LC, and WI38 cells with transfection of pcDNA vector or pcDNA-DHCR24 with or without H_2O_2 treatment are indicated. *Vertical bars*, S.D. *, $p < 0.05$ (two-tailed Student's *t* test). *I*, a caspase 3/7 assay was performed in WI38 cells with pcDNAvector (vector) and pcDNA-DHCR24 overexpression vector. *Vertical bars*, S.D. *, $p < 0.05$ (two-tailed Student's *t* test).

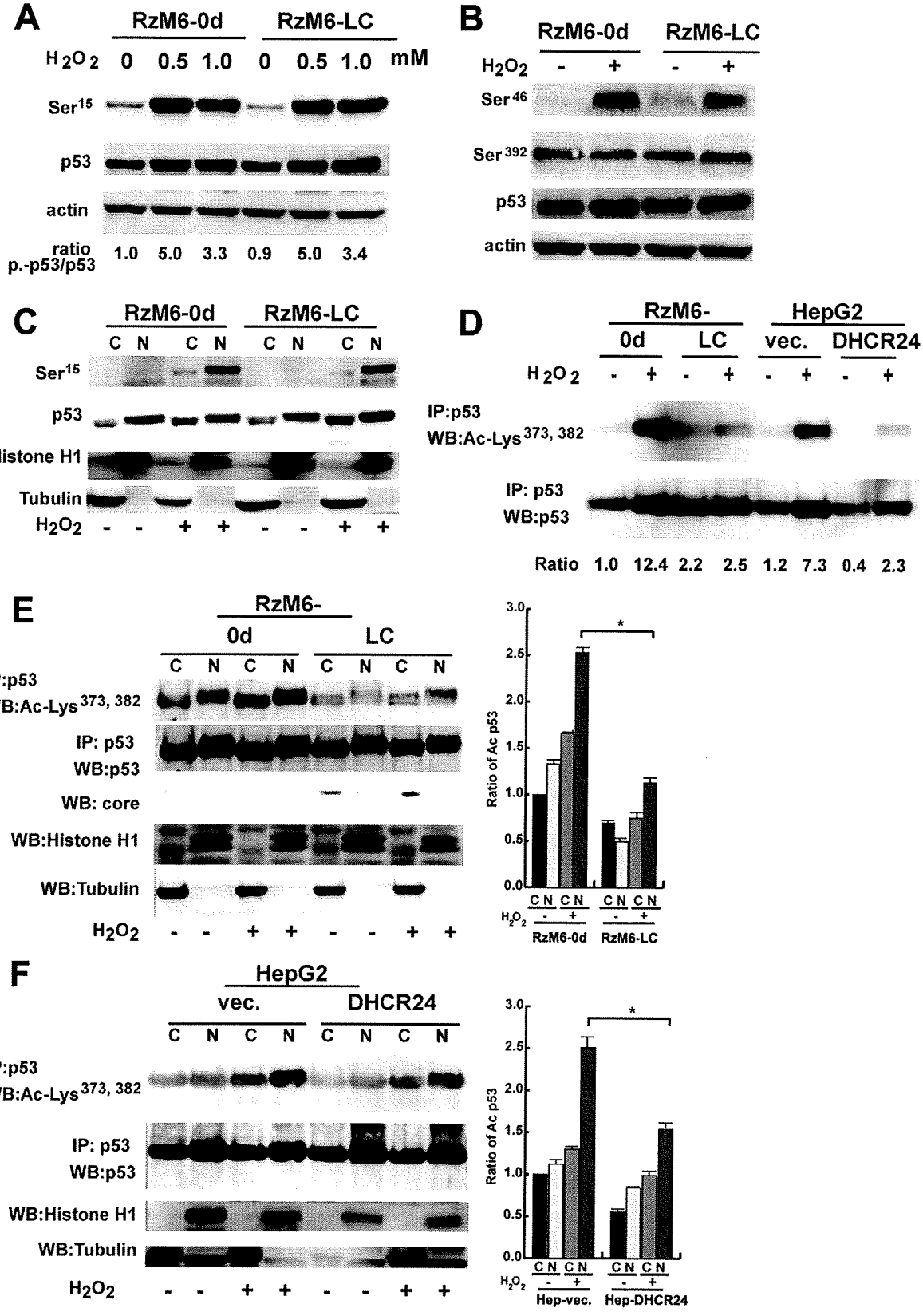

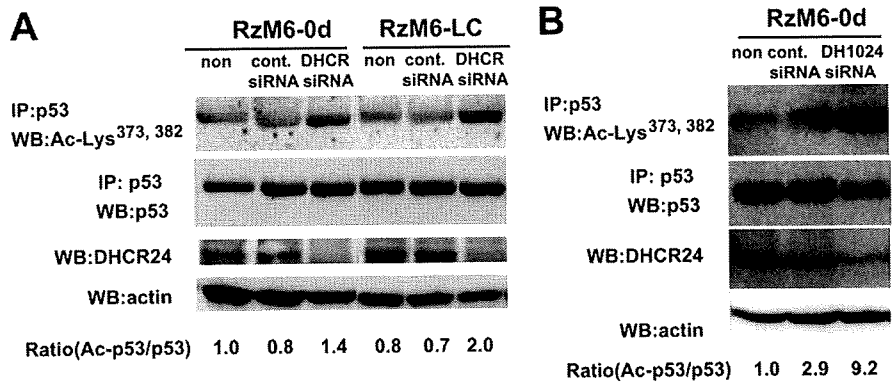

FIGURE 7. **Silencing of DHCR24 increases p53 acetylation.** *A*, RzM6-0d and RzM6-LC cells were untreated (*non*) or treated with control siRNA (*cont. siRNA*) or DHCR24 siRNA. Acetylated p53 Lys^{373} and Lys^{382} (*top*) and total p53 (*bottom*) were immunoprecipitated (*IP*) with anti-p53 antibody (*DO-1*) followed by Western blotting (*WB*), and the expression of actin and DHCR24 by Western blotting (*bottom*) was examined. The average ratio of acetylated p53 to total p53 in RzM6-0d cells without treatment is indicated at the *bottom*. *B*, RzM6-0d cells were transfected with control siRNA (*cont.siRNA*), DHCR24 siRNA (*DH1024* or *DHCR*), or untreated (*non*). Acetylated p53 Lys^{373} and Lys^{382} (*top*) and total p53 (*bottom*) were immunoprecipitated with anti-p53 antibody followed by Western blotting, and the expression of actin and DHCR24 by Western blotting (*bottom*) was examined. Reaction with secondary antibodies (anti-rabbit or mouse IgG conjugated with horseradish peroxidase) alone did not yield any signals (data not shown), and data representative of three independent experiments are shown (*A* and *B*).

treatment (Fig. 5*C*). Silencing of DHCR24 with siRNA decreased the interaction between p53 and MDM2 (supplemental Fig. 2*A*). Overexpression of DHCR24 in HepG2 cells increased the interaction between p53 and MDM2 in the cytoplasm (HepG2-DHCR24; Fig. 5*D* and supplemental Fig. 2, *B* and *C*). Level of p53 in the nucleus after treatment with H_2O_2 was low in RzM6-LC cells (Fig. 5*E*).

In a previous *in vitro* study that used bacterially expressed and purified protein (21), the interaction between p53 and MDM2 was decreased when the amount of DHCR24 was increased. These discrepancies with our results may be due to the different experimental systems. p53 and DHCR24 were induced by H_2O_2 in WI38TERT cells (21), as observed in our system (Fig. 5*F*). However, the interaction between MDM2 and p53 was much lower in WI38 cells than in RzM6 cells (Fig. 5, *G* and *H*). Moreover, ectopic expression of DHCR24 did not inhibit apoptotic response to H_2O_2 in WI38 cells (Fig. 5*I*) but suppressed apoptosis in HepG2 cells (Fig. 3). This different response may be due to the different regulatory systems of p53 and MDM2 in the liver and lung; MDM2 phosphorylation at Ser^{166} is regulated by the MEK-ERK (mitogen-activated protein kinase/extracellular signal-regulated kinase kinase-extracellular signal-regulated kinase) pathway in hepatocytes and Akt in lung cells (29). The response of MDM2 at Ser^{166} to H_2O_2 was significantly high in liver (HepG2) cells but was low in WI38 cells (supplemental Fig. 2, *D* and *E*), as previously observed in A549 cells (29). The up-regulation of MDM2 phosphorylation at Ser^{166} accelerates its E3 ligase activity (30).

We also found that overexpression of DHCR24 did not up-regulate the transcription of *p53* or *MDM2* genes (supplemental Fig. 3, *A* and *B*). However, DHCR24 overexpression inhibited polyubiquitination in RzM6-LC cells and H358 (p53 null) cells (supplemental Fig. 3, *C–E*). This inhibition of polyubiquitination would inhibit p53 degradation, resulting in an increased amount of p53 available to interact with MDM2.

Posttranslational Modification of p53 in DHCR24-overexpressing Cells—We did not detect any *p53* nucleotide substitutions in RzM6-LC cells compared with the *p53* in RzM6-0d cells (data not shown). Thus, we examined the posttranslational modification of p53, which is thought to be tightly connected to the regulation of its function and localization (31). We examined the phosphorylation of p53 at Ser^{15} (Fig. 6*A*); at Ser^{6}, Ser^{9}, Ser^{20}, and Ser^{37} (supplemental Fig. 4*A*); and at Ser^{46} and Ser^{392} (Fig. 6*B*) by Western blotting and found no marked differences in phosphorylation after H_2O_2 treatment between RzM6-0d and RzM6-LC cells. Ser^{15}-phosphorylated p53 was detected in the nuclear fraction of RzM6-0d and RzM6-LC cells after H_2O_2 treatment (Fig. 6*C*). We assessed the acetylation of p53 at Lys^{373} and Lys^{382} by immunoprecipitation followed by Western blotting and found that acetylation of p53 was significantly low in RzM6-LC cells compared with RzM6-0d cells following H_2O_2 treatment (Fig. 6*D*). H_2O_2 induced the acetylation of p53 at Lys^{373} and Lys^{382} in RzM6-0d cells (Fig. 6*E*). This acetylation

FIGURE 6. **Posttranslational modification of p53 in cells overexpressing DHCR24.** *A*, phosphorylation of p53 at Ser^{15} in RzM6-0d and RzM6-LC cells after treatment with 0, 0.5, or 1.0 mM H_2O_2 was examined by Western blotting with specific rabbit polyclonal antibodies. p53 was detected with anti-p53 monoclonal antibody (*DO-1*). Actin was analyzed as a control. *B*, phosphorylation of p53 at Ser^{46} and Ser^{392} in RzM6-0d and RzM6-LC cells after treatment with 0 or 1.0 mM H_2O_2 was analyzed by Western blotting with specific rabbit polyclonal antibodies. p53 was detected with anti-p53 monoclonal antibody. Actin was analyzed as a control. *C*, RzM6-0d or RzM6-LC cells with or without H_2O_2 treatment were fractionated into cytoplasmic (*C*) and nuclear (*N*) fractions that were subjected to Western blotting with the antibodies indicated on the *left*. *D*, acetylation of p53 Lys^{373} and Lys^{382} (*top*) and total p53 (*bottom*) was characterized by immunoprecipitation (*IP*) with anti-p53 antibody followed by Western blotting (*WB*) with the rabbit polyclonal antibodies indicated on the *left* in RzM6-0d and RzM6-LC cells or HepG2 cells transfected with pcDNA vector (*vec.*) or pcDNA-DHCR24 expression vector (*DHCR24*). The average ratio of acetylated p53 to total p53 in RzM6-0d cells without H_2O_2 treatment is indicated at the *bottom*. *E*, acetylation of p53 Lys^{373} and Lys^{382} (*top*) and total p53 (*second panel*) was characterized by immunoprecipitation with anti-p53 antibody followed by Western blotting with the rabbit polyclonal antibodies indicated on the *left* in RzM6-0d and RzM6-LC cells. HCV core protein was detected by Western blotting with monoclonal antibody (31, 32). Cell fractionation was confirmed with antibodies against histone H1 and tubulin. p53 and acetylated p53 were quantitated, and the average ratio of acetylated p53 to total p53 in the cytoplasmic (*C*) fraction of RzM6-0d cells is indicated. *Vertical bars*, S.D. *, $p < 0.05$ (two-tailed Student's *t* test). *F*, acetylation of p53 Lys^{373} and Lys^{382} (*top*) and total p53 (*second panel*) was characterized by IP with anti-p53 antibody followed by Western blotting with the rabbit polyclonal antibodies indicated on the *left* in HepG2 cells transfected with pcDNA vector or pcDNA-DHCR24 vector with or without H_2O_2 treatment. Cell fractionation was confirmed with antibodies against histone H1 and tubulin. p53 and acetylated p53 were quantitated, and the average ratio of acetylated p53 to total p53 in the cytoplasmic fraction of Hep-vec cells is indicated. *Vertical bars*, S.D. *, $p < 0.05$ (two-tailed Student's *t* test). Reaction with secondary antibodies (anti-rabbit or mouse IgG conjugated with horseradish peroxidase) alone did not show any signals (data not shown), and data representative of three independent experiments are indicated (*A–F*).

was significantly inhibited in RzM6-LC cells (Fig. 6*E*). Persistent ectopic overexpression of DHCR24 also repressed H_2O_2-induced p53 acetylation in the nuclei of HepG2 cells (Fig. 6*F*). In addition, silencing of DHCR24 by siRNA caused up-regulation of p53 acetylation at Lys^{373} and Lys^{382} in RzM6-0d and RzM6-LC cells (Fig. 7*A*). When the alternative siRNA for DHCR24 (DH1024) was transfected into RzM6-0d cells, the acetylation of p53 was accelerated (Fig. 7*B*). The mutant DHCR24 vector suppressed the effect of DHCR24 siRNA (supplemental Fig. 4*B*). These results indicate that overexpression of DHCR24 down-regulates p53 acetylation.

DISCUSSION

This study demonstrates that DHCR24 expression parallels hepatocarcinogenesis and that HCV induces overexpression of DHCR24 at both the mRNA and protein levels. Moreover, persistent DHCR24 overexpression suppresses the p53 response to H_2O_2. These findings are consistent with the previous report that inactivation and mutation of p53 plays a role in the development of HCC (32). Hepatocytes with p53 abnormalities are likely to escape from cell cycle check points and acquire resistance to apoptosis, thereby increasing their tumorigenic potential. Likewise, genetic inactivation of p53 is associated with late stage disease (32). HCV RNA levels are notably lower in cancerous tissues from HCV-positive HCC patients than in non-cancerous tissues (33). Thus, impairment of p53 function by HCV-induced DHCR24 overexpression might play a crucial role in early stage disease progression.

In DHCR24-overexpressing cells, p53 was mostly distributed in the cytoplasm (supplemental Fig. 2, *A* and *B*). This change in the distribution pattern of p53 might be caused by an increased interaction between p53 and MDM2, which might be induced by increased phosphorylation of MDM2 and suppression of polyubiquitination by overexpression of DHCR24. The up-regulation of the p53-MDM2 interaction negatively regulates p53 and shuttles p53 from the nucleus to the cytoplasm (34, 35). MDM2 inhibits both *p53* transcriptional activation and p300-mediated p53 acetylation upon ternary complex formation with p300 and p53 (36–38). Acetylation of p53 by CBP/p300 mostly occurs in the nucleus (36). Therefore, the increase in cytoplasmic p53-MDM2 complexes in DHCR24-overexpressing cells may account for the observed suppression of p53 acetylation in the nucleus, even after treatment with H_2O_2 (supplemental Fig. 5). Impaired acetylation of C-terminal lysine residues decreases the sequence-specific DNA-binding activity (39) and the stability of p53 (37, 40). Taken together, our data suggest that DHCR24 overexpression may down-regulate p53 function by inhibiting degradation, increasing the formation of the p53-MDM2 complex in the cytoplasm, and suppressing acetylation of p53 in the nucleus.

In conclusion, we propose that HCV infection impairs the function of p53 through DHCR24 overexpression, which up-regulates the interaction between p53 and MDM2 in the cytoplasm and suppresses p53 acetylation in the nucleus. Because overexpression of DHCR24 is observed in other cancers, including melanoma (24) and prostate cancer (41), the findings from this study might provide a foundation for investigations into the mechanisms underlying the formation of these cancers. We plan to examine the liver-specific regulatory network of the p53-MDM2 interaction by DHCR24 in a future study.

Acknowledgments—We thank S. Imajoh-Ohmi, H. Fukuda, T. Watanabe, S. Nakagawa, K. Tanaka, and R. Takehara for technical support and N. Sonenberg, Y. Furuichi, T. Tsukiyama, S. Tone, S. Sekiguchi, and F. Yasui for valuable comments. We thank S. Harada (Kumamoto University) for kind encouragement.

REFERENCES

1. Choo, Q. L., Kuo, G., Weiner, A. J., Overby, L. R., Bradley, D. W., and Houghton, M. (1989) *Science* **244,** 359–362
2. Tsukiyama-Kohara, K., Iizuka, N., Kohara, M., and Nomoto, A. (1992) *J. Virol.* **66,** 1476–1483
3. Grakoui, A., Wychowski, C., Lin, C., Feinstone, S. M., and Rice, C. M. (1993) *J. Virol.* **67,** 1385–1395
4. Pekow, J. R., Bhan, A. K., Zheng, H., and Chung, R. T. (2007) *Cancer* **109,** 2490–2496
5. Lauer, G. M., and Walker, B. D. (2001) *N. Engl. J. Med.* **345,** 41–52
6. Saito, I., Miyamura, T., Ohbayashi, A., Harada, H., Katayama, T., Kikuchi, S., Watanabe, Y., Koi, S., Onji, M., Ohta, Y., *et al.* (1990) *Proc. Natl. Acad. Sci. U.S.A.* **87,** 6547–6549
7. Shepard, C. W., Finelli, L., and Alter, M. J. (2005) *Lancet Infect. Dis.* **5,** 558–567
8. Kiyosawa, K., Umemura, T., Ichijo, T., Matsumoto, A., Yoshizawa, K., Gad, A., and Tanaka, E. (2004) *Gastroenterology* **127,** S17–S26
9. Parkin, D. M. (2001) *Lancet Oncol.* **2,** 533–543
10. Hussain, S. P., Schwank, J., Staib, F., Wang, X. W., and Harris, C. C. (2007) *Oncogene* **26,** 2166–2176
11. Tardif, K. D., Waris, G., and Siddiqui, A. (2005) *Trends Microbiol.* **13,** 159–163
12. Levrero, M. (2006) *Oncogene* **25,** 3834–3847
13. Tsukiyama-Kohara, K., Toné, S., Maruyama, I., Inoue, K., Katsume, A., Nuriya, H., Ohmori, H., Ohkawa, J., Taira, K., Hoshikawa, Y., Shibasaki, F., Reth, M., Minatogawa, Y., and Kohara, M. (2004) *J. Biol. Chem.* **279,** 14531–14541
14. Köhler, G., and Milstein, C. (1975) *Nature* **256,** 495–497
15. Yasui, K., Wakita, T., Tsukiyama-Kohara, K., Funahashi, S. I., Ichikawa, M., Kajita, T., Moradpour, D., Wands, J. R., and Kohara, M. (1998) *J. Virol.* **72,** 6048–6055
16. Tsukiyama-Kohara, K., Poulin, F., Kohara, M., DeMaria, C. T., Cheng, A., Wu, Z., Gingras, A. C., Katsume, A., Elchebly, M., Spiegelman, B. M., Harper, M. E., Tremblay, M. L., and Sonenberg, N. (2001) *Nat. Med.* **7,** 1128–1132
17. Watanabe, T., Sudoh, M., Miyagishi, M., Akashi, H., Arai, M., Inoue, K., Taira, K., Yoshiba, M., and Kohara, M. (2006) *Gene. Ther.* **13,** 883–892
18. Iivonen, S., Hiltunen, M., Alafuzoff, I., Mannermaa, A., Kerokoski, P., Puoliväli, J., Salminen, A., Helisalmi, S., and Soininen, H. (2002) *Neuroscience* **113,** 301–310
19. Greeve, I., Hermans-Borgmeyer, I., Brellinger, C., Kasper, D., Gomez-Isla, T., Behl, C., Levkau, B., and Nitsch, R. M. (2000) *J. Neurosci.* **20,** 7345–7352
20. Waterham, H. R., Koster, J., Romeijn, G. J., Hennekam, R. C., Vreken, P., Andersson, H. C., FitzPatrick, D. R., Kelley, R. I., and Wanders, R. J. (2001) *Am. J. Hum. Genet.* **69,** 685–694
21. Wu, C., Miloslavskaya, I., Demontis, S., Maestro, R., and Galaktionov, K. (2004) *Nature* **432,** 640–645
22. Wakita, T., Pietschmann, T., Kato, T., Date, T., Miyamoto, M., Zhao, Z., Murthy, K., Habermann, A., Kräusslich, H. G., Mizokami, M., Bartenschlager, R., and Liang, T. J. (2005) *Nat. Med.* **11,** 791–796
23. Kuehnle, K., Crameri, A., Kälin, R. E., Luciani, P., Benvenuti, S., Peri, A., Ratti, F., Rodolfo, M., Kulic, L., Heppner, F. L., Nitsch, R. M., and Mohajeri, M. H. (2008) *Mol. Cell. Biol.* **28,** 539–550
24. Di Stasi, D., Vallacchi, V., Campi, V., Ranzani, T., Daniotti, M., Chiodini, E., Fiorentini, S., Greeve, I., Prinetti, A., Rivoltini, L., Pierotti, M. A., and Rodolfo, M. (2005) *Int. J. Cancer* **115,** 224–230
25. Lois, C., Hong, E. J., Pease, S., Brown, E. J., and Baltimore, D. (2002) *Science*

295, 868–872
26. Yamamoto, H., Ozaki, T., Nakanishi, M., Kikuchi, H., Yoshida, K., Horie, H., Kuwano, H., and Nakagawara, A. (2007) *Genes Cells* **12,** 461–471
27. Miyashita, T., and Reed, J. C. (1995) *Cell* **80,** 293–299
28. Yu, J., Zhang, L., Hwang, P. M., Kinzler, K. W., and Vogelstein, B. (2001) *Mol. Cell* **7,** 673–682
29. Malmlöf, M., Roudier, E., Högberg, J., and Stenius, U. (2007) *J. Biol. Chem.* **282,** 2288–2296
30. Gottlieb, T. M., Leal, J. F., Seger, R., Taya, Y., and Oren, M. (2002) *Oncogene* **21,** 1299–1303
31. Bode, A. M., and Dong, Z. (2004) *Nat. Rev. Cancer* **4,** 793–805
32. Farazi, P. A., and DePinho, R. A. (2006) *Nat. Rev. Cancer* **6,** 674–687
33. Tanaka, T., Inoue, K., Hayashi, Y., Abe, A., Tsukiyama-Kohara, K., Nuriya, H., Aoki, Y., Kawaguchi, R., Kubota, K., Yoshiba, M., Koike, M., Tanaka, S., and Kohara, M. (2004) *J. Med. Virol.* **72,** 223–229
34. Roth, J., Dobbelstein, M., Freedman, D. A., Shenk, T., and Levine, A. J. (1998) *EMBO J.* **17,** 554–564
35. Freedman, D. A., and Levine, A. J. (1998) *Mol. Cell. Biol.* **18,** 7288–7293
36. Kobet, E., Zeng, X., Zhu, Y., Keller, D., and Lu, H. (2000) *Proc. Natl. Acad. Sci. U.S.A.* **97,** 12547–12552
37. Ito, A., Lai, C. H., Zhao, X., Saito, S., Hamilton, M. H., Appella, E., and Yao, T. P. (2001) *EMBO J.* **20,** 1331–1340
38. Ohkubo, S., Tanaka, T., Taya, Y., Kitazato, K., and Prives, C. (2006) *J. Biol. Chem.* **281,** 16943–16950
39. Gu, W., and Roeder, R. G. (1997) *Cell* **90,** 595–606
40. Yuan, Z. M., Huang, Y., Ishiko, T., Nakada, S., Utsugisawa, T., Shioya, H., Utsugisawa, Y., Yokoyama, K., Weichselbaum, R., Shi, Y., and Kufe, D. (1999) *J. Biol. Chem.* **274,** 1883–1886
41. Bonaccorsi, L., Luciani, P., Nesi, G., Mannucci, E., Deledda, C., Dichiara, F., Paglierani, M., Rosati, F., Masieri, L., Serni, S., Carini, M., Proietti-Pannunzi, L., Monti, S., Forti, G., Danza, G., Serio, M., and Peri, A. (2008) *Lab. Invest.* **88,** 1049–1056

Antiviral Research 83 (2009) 112–117

Contents lists available at ScienceDirect

Antiviral Research

journal homepage: www.elsevier.com/locate/antiviral

Identification of bisindolylmaleimides and indolocarbazoles as inhibitors of HCV replication by tube-capture-RT-PCR

Yuko Murakami[a,*], Kohji Noguchi[a], Satoshi Yamagoe[a], Tetsuro Suzuki[b], Takaji Wakita[b], Hidesuke Fukazawa[a,*]

[a] Department of Bioactive Molecules, National Institute of Infectious Diseases, Toyama 1-23-1, Shinjuku-ku, Tokyo 162-8640, Japan
[b] Department of Virology II, National Institute of Infectious Diseases, Tokyo, Japan

ARTICLE INFO

Article history:
Received 31 July 2008
Received in revised form 10 February 2009
Accepted 27 March 2009

Keywords:
HCV
Bisindolylmaleimide
Tube-capture-RT-PCR
High-throughput

ABSTRACT

We devised a screening method for hepatitis C virus (HCV) inhibitors by exploiting the JFH1 viral culture system. The viral RNA released in the medium was adsorbed onto PCR plates, and real-time RT-PCR was performed by directly adding the one-step RT-PCR reaction mixture to the wells. The "tube-capture-RT-PCR" method obviates the need for labor-intensive RNA isolation and should allow high-throughput screening of HCV inhibitors. To substantiate the validity of the assay for drug screening, a pilot screen of an inhibitor library composed of 95 compounds was performed. In addition to the known inhibitors of HCV replication included in the library, the assay identified the PKC inhibitor bisindolylmaleimide I (BIM I) as an HCV replication inhibitor. BIM I was also effective in reducing the viral protein level in genotype 1b and 2a subgenomic replicon cells, indicating inhibition of HCV replication. Further assays revealed that a broad range of bisindolylmaleimides and indolocarbazoles inhibit HCV, but no correlation was found between the PKC inhibition pattern and anti-HCV activity. These series of compounds represent new classes of inhibitors that may warrant further development.

1. Introduction

Hepatitis C virus, a major cause of chronic liver disease, has infected over 170 million people. The current mainstream anti-HCV therapy is a combination of interferon (IFN) and ribavirin. However, the therapy is not effective in approximately half of HCV-infected patients and has considerable side effects in many patients; thus, there is an urgent need for novel HCV therapies.

Various assays for HCV drug screening have been reported, many of which rely on HCV replicon systems. Although HCV replicon-based systems have greatly facilitated HCV research and drug discovery, these systems do not completely reflect the entire HCV life cycle and are not capable of identifying inhibitors of several important steps such as viral attachment, entry, and release. The recently introduced HCV cell culture systems (Wakita et al., 2005) should overcome these limitations and enable identification of inhibitors that would not be recognized by the replicon-based screens.

Here we describe a simple screening method for discovering anti-HCV drugs using the JFH1 viral culture system. Antiviral activity was determined by RT-PCR measurement of viral RNA released in the medium of infected cells. To increase efficiency, we devised a method that avoids tedious RNA isolation.

As a proof of concept, the method was used to evaluate a compound library and successfully confirmed the anti-HCV activity of cyclosporin A. In addition, a potent and selective PKC inhibitor, BIM I, was also identified as an anti-HCV agent. We found that other bisindolylmaleimides and indolocarbazoles also inhibit HCV, whereas anti-HCV activity was not associated with PKC inhibition. HCV inhibition by bisindolylmaleimides or indolocarbazoles has not been reported, and we expect that our assay will facilitate the identification of previously unrecognized HCV inhibitors. The bisindolylmaleimides and indolocarbazoles are already in clinical trials and may merit attention as HCV drug candidates.

2. Materials and methods

2.1. Cells and virus

Plasmid pJFH1, containing full-length cDNA of the JFH1 isolate, was used to generate HCV production in cell culture, as described elsewhere (Wakita et al., 2005), and the supernatant was passaged in Huh 7.5.1 cells. To prepare virus stock for screening, naïve Huh 7.5.1 cells were infected with the passaged supernatant virus, and the medium was collected 7 days post-infection and stored at

* Corresponding authors. Tel.: +81 3 5285 1111x2327; fax: +81 3 5285 1272.
E-mail addresses: murakami@nih.go.jp (Y. Murakami), fukazawa@nih.go.jp (H. Fukazawa).

0166-3542/$ – see front matter © 2009 Elsevier B.V. All rights reserved.
doi:10.1016/j.antiviral.2009.03.008

−80 °C until use. The infectious titers of the viruses were determined by immunofluorescence analysis of the infected Huh 7.5.1 cells using anti-core antibody (2H9). The infectious titers of the stocks were generally about 3×10^5–1×10^6 ffu/ml, corresponding to about 3×10^7–1×10^8 copies of JFH1 RNA/ml. A subgenomic replicon cell, clone 4-1, which harbors the genotype 2a HCV genome (Kato et al., 2003; Date et al., 2004) and clone 5-15, which harbors the genotype 1b HCV genome (Lohmann et al., 1999), were also cultured in Dulbecco's Modified Eagle's medium (DMEM) with fetal bovine serum (FBS).

2.2. Reagents

The SCADS inhibitor kit I was provided by the Screening Committee of Anticancer Drugs supported by a Grant-in-Aid for Scientific Research on the Priority Area "Cancer" from The Ministry of Education, Culture, Sports, Science and Technology, Japan. The PKC β isozyme selective inhibitor LY333531 (Ruboxistaurin) was from Alexis Corp. (Lausen, Switzerland). Other chemicals were purchased from Merck Calbiochem (Darmstadt, Germany). Interferon-α (IFN-α) was from PeproTech, Inc. (Princeton Business Park, Princeton, NJ).

2.3. Quantitative real-time RT-PCR

Huh 7.5.1. cells were seeded in 96-well plates at a density of 20,000 cells per well in a volume of 120 μl. The next day, 15 μl of test compounds was added and the cells were infected with 15 μl of virus stock of HCV-JFH1 at a multiplicity of infection (MOI) of 0.01. After 5 days of culture, 100 μl of medium was transferred to a PCR plate, incubated on ice for 30 min, centrifuged at 3500 rpm for 15 min, and then removed. Twenty microliters of One Step SYBR PrimeScript RT-PCR Kit reaction mixture (Takara-Bio Co., Otsu, Japan) was added into the PCR plate wells, and quantitative real-time PCR was performed using an ABI Prism 7000 sequence detector (PE Applied Biosystems, Foster City, CA). The primers used were 5′-GAGTGTCGTACAGCCTCCAG-3′ (nucleotides 97–116), and 5′-AGGCCTTTCGCAACCCA-3′ (nucleotides 280–264) from the noncoding region of HCV-JFH1, at a concentration of 200 nM. Media from the control wells without drug were serially diluted to create a standard curve, which was used to determine the relative amount of HCV RNA in the media of HCV-infected cells treated with the compounds. Cell growth was monitored by MTT assay, as described previously (Fukazawa et al., 1995).

For further analysis of the drug effect and determination of the copy number of HCV RNA in medium and cells, HCV RNA was extracted from 140 μl medium with the QIAamp Viral RNA mini kit (QIAGEN GmbH, Hilden, Germany), and eluted with 60 μl of elution buffer. Eight microliters of the viral RNA eluate was subjected to quantitative real-time PCR using Taqman EZ RT-PCR Core reagents (PE Applied Biosystems). The primers were 5′-CGGGAGAGCCATAGTGG (nucleotides 129–145) and 5′-AGTACCACAAGGCCTTTCG (nucleotides 289–271) at a concentration of 200 nM, and the Taqman probe was FAM-5′-CTGCGGAACCGGTGAGTACAC-3′-TAMRA (nucleotides 147–167) at a concentration of 300 nM (Takeuchi et al., 1999). Standard JFH1 RNA for measurement of copy number was transcribed from plasmid pSRG-JFH1-Luci, which was derived from pSRG-JFH1 (Kato et al., 2003), using the AmpliScribe T7 High Yield Transcription Kit (Epicentre Biotechnologies, Madison, WI). The transcribed RNA was purified and diluted with ribonuclease-free water containing yeast tRNA and 0.2% DTT, as previously described (Suzuki et al., 2005).

2.4. Western blotting

Cells were lysed with Radio-ImmunoPrecipitation Assay (RIPA) buffer (50 mM Tris–HCl, pH 8.0, 150 mM NaCl, 0.1% SDS, 0.5% sodium deoxycholate, 1% NP-40, 1 mM EDTA) containing 1 mM phenylmethylsulfonyl fluoride (PMSF) and 25 μg/ml of each of antipain, pepstatin, and leupeptin, and centrifuged. The amount of protein in the supernatant was then measured. Cell lysates containing equal amounts of protein were separated by SDS-PAGE, transferred onto polyvinylidene difluoride (PVDF) membranes, and probed with antibodies against core (2H9), NS5A (Austral Biologicals, San Raman, CA), α-tubulin (Merck Calbiochem), and GAPDH (Santa Cruz Biotech. Inc., Santa Cruz, CA). The membranes were incubated with horseradish peroxidase-conjugated secondary antibodies and specific proteins were visualized by chemiluminescence.

3. Results

3.1. Assay development

To establish an efficient RT-PCR-based screen for anti-HCV agents, we searched for methods that could be carried out without labor-intensive RNA isolation. We tested whether tube-trapping methods used to obtain plant viral RNAs for RT-PCR (Rowhani et al., 1995; James, 1999; Suehiro et al., 2005) could be applied to HCV. A JFH1 stock solution (3×10^5 ffu/ml, 3×10^7 copies/ml) was serially diluted fourfold, put into the wells of the PCR plate, incubated on ice for 30 min, and then centrifuged at 3500 rpm for 15 min. The supernatant was removed and quantitative RT-PCR was performed by direct addition of the one-step RT-PCR reaction mixture. We found that HCV, like plant viruses, are adsorbed onto the well wall during incubation. As shown in Fig. 1a, RNA adsorption appeared to be linear over a broad range of viral concentrations. HCV RNA could still be detected after seven fourfold dilutions, indicating that the "tube-capture" is a quantitative method that can detect less than 200 copies of HCV RNA. We compared the CT values from this "tube-capture method" with those from the conventional method of RNA extraction. The efficiency of RNA recovery by "tube-capture" was calculated to be about 9% of the conventional method. However, as shown in Fig. 1a, there was a close correlation between the CT values obtained from the two methods ($R = 0.988$), demonstrating the usefulness of this method.

3.2. Identification of BIM I as an inhibitor of HCV infection

To explore the possibility of tube-capture-RT-PCR as a simple screen for discovering anti-HCV compounds, we first tested whether the method would detect the antiviral activity of IFN-α. Huh7.5.1 cells were seeded in a 96-well plate and infected with HCV-JFH1 at an MOI of 0.01. After 5 days, HCV RNA released in the medium was assayed by the tube-capture method. Under these conditions, the CT from the control medium was usually about 18–20. As shown in Fig. 1b, a substantial reduction in the amount of HCV RNA was observed when the cells were infected in the presence of IFN-α.

For further validation of the ability of the assay to identify HCV inhibitors, we performed a pilot screen using an inhibitor kit provided by the Screening Committee of Anticancer Drugs (SCADS inhibitor kit I). This kit contains 95 inhibitors including cyclosporin A, a compound reported to inhibit HCV replication.

Cyclosporin A was identified (Fig. 1c), providing a proof of concept for screening for anti-HCV drug candidates. In addition, our assay also identified the PKC inhibitor bisindolylmaleimide I (BIM I) (Fig. 2a, black columns). The IC_{50} was about 0.1 μM, which is comparable to that of cyclosporin A and about 200-fold lower than the IC_{50} for cell growth (Fig. 2b). In addition, BIM I inhibited the cytopathic effect of HCV JFH1. Infection with HCV resulted in about a 20% reduction of cell growth. BIM I at 1 μM enhanced the growth of

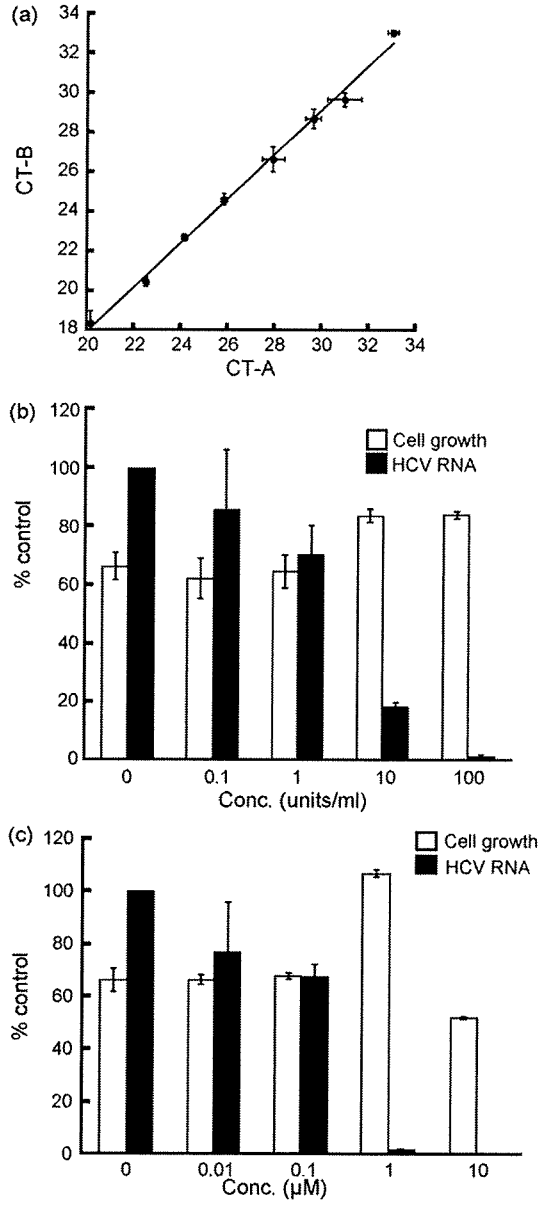

Fig. 1. RT-PCR-based screen for anti-HCV agents using the JFH1 viral culture system. (a) Correlation between CT values from "tube-capture-RT-PCR" (CT-A) and ordinary RNA extraction (CT-B). JFH1 stock solution (3×10^5 ffu/ml) was serially diluted four-fold and quantitative real-time PCR was performed as described under Section 2. CT-A was the average CT of three wells using tube-capture-RT-PCR and CT-B was the average CT of three HCV RNA eluates using a kit (QIAamp Viral RNA mini). (b) and (c) Huh 7.5.1 cells were infected with JFH1 in the presence of the indicated concentrations of IFN-α (b) or cyclosporin A (c). HCV RNA in the medium (closed (black) columns) was assessed by "tube-capture-RT-PCR" as described under Section 2. Open (white) columns represent percentage of cell growth compared with that of control cells without virus and compound. Columns, mean of triplicate wells; bars, SD.

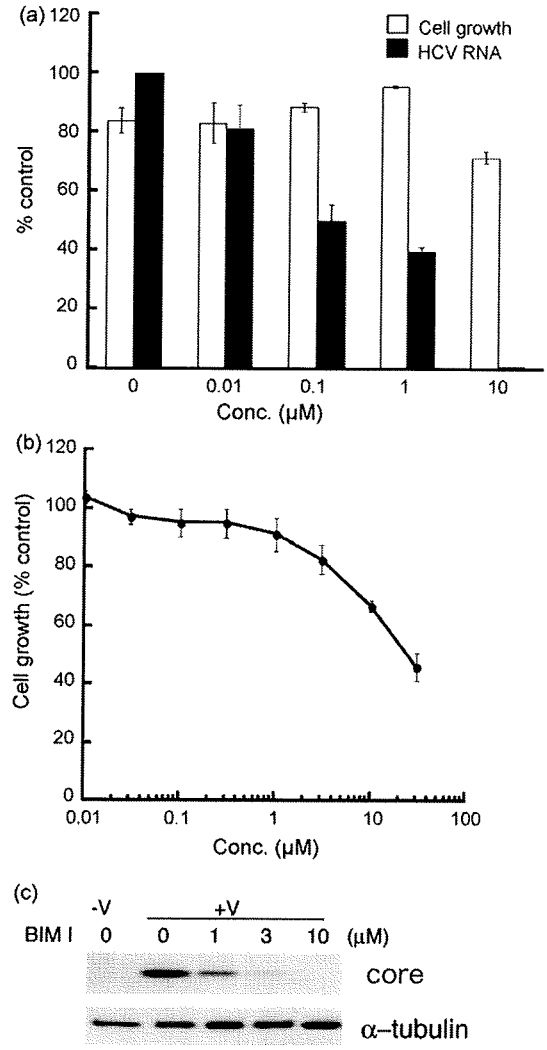

Fig. 2. BIM I inhibits HCV. (a) Effects of BIM I on HCV JFH1 RNA. Huh 7.5.1 cells were infected with JFH1 in the presence of the indicated concentrations of BIM I and assayed for HCV RNA and cell growth as in Fig. 1. Columns, mean of triplicate wells; bars, SD. (b) Effects of BIM I on growth of Huh 7.5.1 cells. (c) Effects of BIM I on HCV core protein in cells. Cells were infected with JFH1 at an MOI of 0.2 in the presence of the indicated concentrations of BIM I and cultured for 2 days. Cells were lysed and subjected to western blotting as described under Section 2. "V" indicates infection with HCV.

infected cells, almost to the level of uninfected cells (Fig. 2a, white columns). Recovery of cell growth was also observed with INF-α or cyclosporin A treatment (Fig. 1b and c). BIM I reduced cell growth of uninfected cells only at concentrations of 1 μM or higher (Fig. 2b). BIM I also inhibited the production of the HCV core protein with marginal effects on host α-tubulin levels (Fig. 2c).

3.3. *BIM I inhibits HCV replication*

To our knowledge, the anti-HCV effects of BIM I or other PKC inhibitors have not been reported. Because the majority of current HCV drug screening relies on replicon-based models, we investigated the possibility that BIM I targets a step in the HCV life cycle that is not included in the replicon systems, such as attachment, entry or release. We treated two subgenomic replicon cells with BIM I and examined the amount of NS5A protein.

As shown in Fig. 3a and b, BIM I dose-dependently reduced NS5A in both 1b and 2a subgenomic replicon cells, but not the host GAPDH. The results indicate that BIM I inhibits a process involved in the replication of HCV subgenomic replicons. However, although the NS5A level appeared to be more vulnerable, cell growth was substantially suppressed by BIM I (Fig. 3c). Whereas a significant difference between the IC_{50} for HCV RNA and cell growth was observed in the HCV cell culture system, the reduction of NS5A in replicon cells overlapped with the effects on cell growth.

To further elucidate the stage of the HCV life cycle affected by BIM I, Huh 7.5.1 cells were inoculated with higher titers of JFH1 (MOI 2) and then treated with 3 μM BIM I, starting at different time points after infection. JFH1 appeared to complete the life cycle in about 48 h, judging from the expression profiles of viral RNA and proteins in cells (Fig. 4a). When BIM I was added at the time of infection,

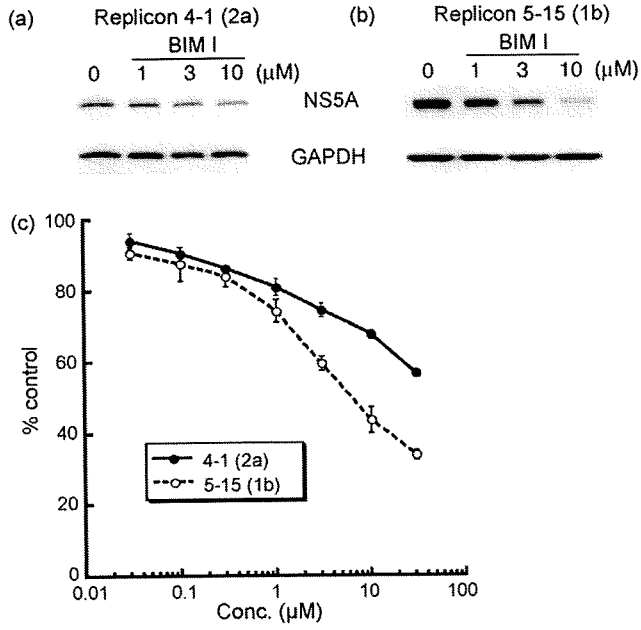

Fig. 3. Effect of BIM I on subgenomic replicon cells. (a) Subgenomic replicon cells harboring genotype 2a (4-1) (a) and genotype 1b (5-15) (b) were treated with BIM I for 2 or 4 days, respectively. Cells were lysed and analyzed by western blotting with anti-NS5A antibody or anti-GAPDH antibody. (c) Effect of BIM I on cell growth of the two replicon cells. Cells were incubated for 2 (4-1) or 4 days (5-15) with BIM I, and cell growth was measured by MTT assay.

the amount of viral RNA in the medium after 48 h decreased to less than 20% of control cells without inhibitor treatment. Addition of BIM I at 6 h post-infection still resulted in a reduction of viral RNA to 30% of control, but after 24 h the antiviral activity of BIM I was significantly diminished and only a modest decline to about 80% was observed (Fig. 4b). These results suggest that interference with RNA synthesis or translation of viral proteins accounts, at least in part, for the anti-HCV activity of BIM I.

3.4. *HCV inhibition by bisindolylmaleimide and indolocarbazole compounds does not involve PKC*

Since the discovery of staurosporine as a broad-spectrum protein kinase inhibitor, a variety of bisindolylmaleimide and indolocarbazole inhibitors with different potencies and selectivity have been developed. BIM I is one such compound that is highly specific for PKC and is broadly used to analyze PKC-mediated events. To gain insight into the relevance of the PKC inhibitory spectrum and antiviral activity, panels of different bisindolylmaleimide and indolocarbazole compounds were tested in the assays. Contrary to our expectation, no correlation was found between the ability to inhibit PKC and HCV.

Another bisindolylmaleimide PKC inhibitor without the N-dimethylaminopropyl chain, BIM IV, displayed similar significant anti-HCV activity (Fig. 5). Other structurally related pan- and isozyme-specific PKC inhibitors such as BIM II, Ro31-8220 (BIM IX), LY333,531 and 3-(1-(3-imidazol-1-ylpropyl)-1H-indol-3-yl)-4-anilino-1H-pyrrole-2,5-dione (PKCβ Inhibitor, Calbiochem) or an indolocarbazole compound K252c also inhibited HCV replication (not shown). However, as shown in Fig. 5, the non-PKC-inhibitory analog BIM V (Toullec et al., 1991) and arcyriaflavin A, an indolocarbazole compound with no reported effects on PKC (Zhu et al., 2003), were also effective in reducing HCV RNA. BIM V was actually more potent than BIM I. Whereas the effect of BIM I on HCV overlapped with cytotoxicity in this particular experiment, BIM V was virtually nontoxic at a dose (1 μM) that reduced

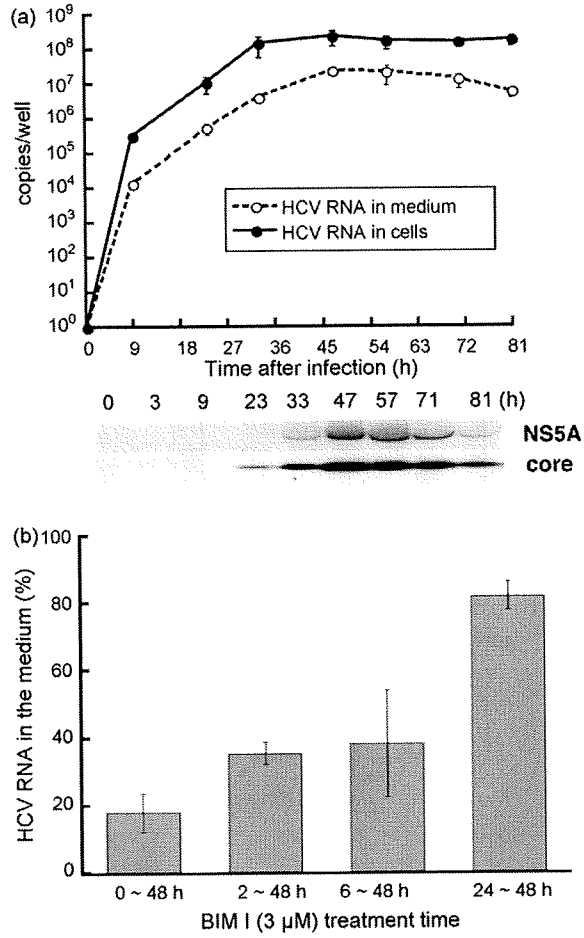

Fig. 4. (a) Expression profile of the HCV RNA and proteins. Huh 7.5.1 cells were infected with HCV as described above, but at an MOI of 2. The cells and medium were harvested at the indicated time and analyzed for HCV RNA and proteins. The core and NS5A protein were detected in the cell lysate. (b) Effect of time of addition. BIM I (3 μM) was added to Huh 7.5.1 cells just before and 2, 6, or 24 h after HCV addition at an MOI of 0.2. After 48 h of incubation following virus infection, the HCV RNA in the medium was extracted and measured with quantitative real-time RT-PCR. The indicated values represent the averages for two independent experiments.

HCV RNA to less than 20% of control. The results indicate that a broad range of bisindolylmaleimide and indolocarbazole compounds inhibit HCV replication, albeit in a PKC-independent manner.

4. Discussion

HCV replicon systems have made significant contributions in HCV research and drug development. Nevertheless, as drug screening tools, replicon systems have limitations because they are not capable of identifying inhibitors of several important events in the viral life cycle. The use of HCV cell culture systems should overcome the drawbacks of the replicon systems and facilitate the identification of inhibitors with novel mechanisms of action. Actually, it has recently been shown that use of an infectious HCV system identified inhibitors that a replicon-based screen did not recognize (Zhang et al., 2008).

We developed a simple screening method for HCV inhibitors that measures the viral RNA released from JFH1-infected cells. The assay does not require specially engineered viruses. The "tube-capture-RT-PCR" method obviates the need for labor-intensive RNA isolation and significantly increases the efficiency of screening. The validity of the assay was confirmed by successful identification of known

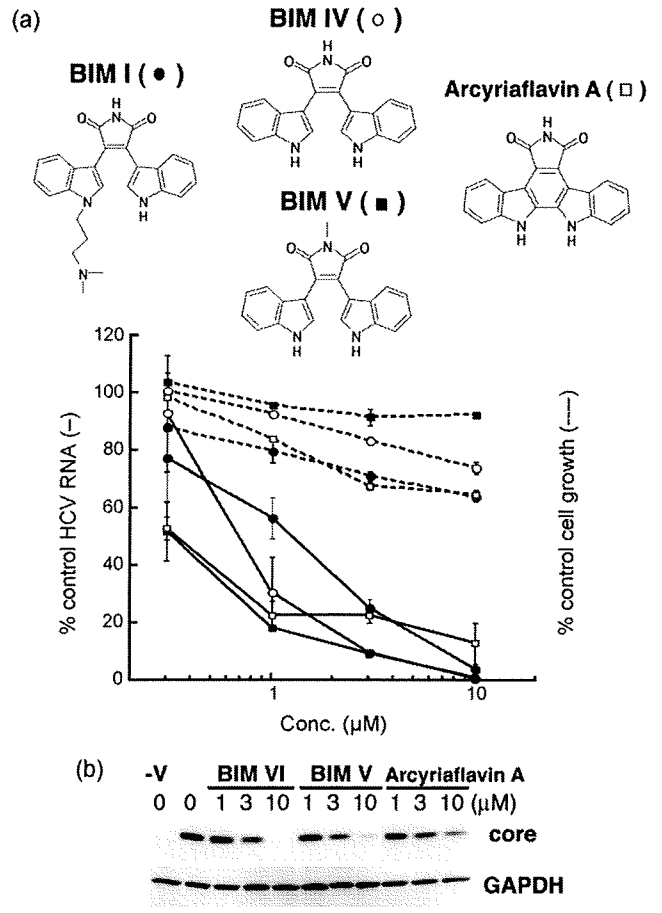

Fig. 5. Effects of bisindolylmaleimide or indolocarbazole compounds on HCV infection. (a) Effects of BIM I, BIM IV, BIM V, and arcyriaflavin A on HCV RNA in the medium. Huh 7.5.1 cells were seeded and infected with HCV at an MOI of 0.01 in the presence of drugs. After 4 days of incubation, the HCV RNA in the medium was extracted and quantified. The relative amounts of HCV RNA with BIM I (closed circle), BIM IV (open circle), BIM V (closed rectangle), and arcyriaflavin A (open rectangle) are represented by solid lines. Cell viability, represented by dotted lines, was determined by MTT assay of a parallel culture without HCV challenge. (b) Effects of BIM IV, BIM V and arcyriaflavin A on core proteins in cells. The cells were infected with JFH1 at an MOI of 0.2 in the presence of the indicated concentrations of compounds and analyzed as described in Fig. 2c. "–V" indicates control without HCV infection.

HCV inhibitors in the pilot screen. In addition, the assay identified the PKC inhibitor BIM I.

BIM I is a widely used compound, and it was somewhat surprising to us that its anti-HCV activity had not been reported. HCV replication in the cell culture system appeared to be considerably more susceptible to BIM I than in the replicon systems, and this is probably why this compound had not been identified as an HCV inhibitor.

Because virus replication is closely linked to host cell growth, HCV inhibition could occur as a result of cell growth inhibition. However, as shown in Fig. 2a, BIM I reduced the cytopathic effect of HCV infection just like interferon-α and cyclosporin A. BIM I, at 1 μM, enhanced the growth of infected cells almost to the level of uninfected cells, presumably because HCV replication, but not cell growth, was inhibited, resulting in a reversal of the cytopathic effect.

Because the PKC inhibitory properties of bisindolylmaleimides and indolocarbazoles have been characterized extensively, we tested a panel of commercially available compounds in the assay to gain insight into the role of PKC in HCV replication. However, no correlation between PKC inhibition and antiviral activity could be found. Anti-HCV activity did not involve PKC inhibition, apparently because a non-PKC-inhibitory analog, BIM V, was also active. Furthermore, PKC inhibitors with different structures, such as calphostin C and H-7, did not show specific inhibition of HCV (data not shown).

Previous studies have indicated that bisindolylmaleimide PKC inhibitors have cellular targets other than PKC. It has been shown that BIM I and Ro31-8220 inhibit p70S6K and p90RSK (Alessi, 1997; Roberts et al., 2005) and that BIM V inhibits p70S6K (Marmy-Conus et al., 2002). Although we did not monitor the activities of these enzymes in our experiments, inhibition of p70S6K is unlikely to be responsible for the anti-HCV effect of PKC inhibitors, because Ishida et al. reported that silencing of p70S6K enhanced HCV RNA abundance (Ishida et al., 2007).

Bisindolylmaleimides and indolocarbazoles have also been reported to inhibit the ATP-binding cassette (ABC) transporters P-glycoprotein and multidrug resistance-associated protein 1 (MRP1), efflux pumps that play important roles in cancer drug resistance (Merritt et al., 1999; Gekeler et al., 1995). More recently, Robey et al. reported that BIMs I, II, III, IV, and V, K252c, and arcyriaflavin A inhibit ABCG2, an ABC half-transporter that confers resistance to various antitumor agents (Robey et al., 2007). Whether ABC transporters play any role in HCV infection awaits further study. We are currently examining the anti-HCV effects of other ABC transporter inhibitors.

In conclusion, we developed a simple infectious HCV system-based assay that can be used for high-throughput screening of HCV inhibitors and identified bisindolylmaleimides and indolocarbazoles. These compounds might represent lead substances for the development of new HCV drugs. Further analysis of the mechanism of HCV-inhibition by these compounds might reveal a new mechanism of regulation of HCV infection.

Acknowledgments

We thank Drs. Kyoko Murakami, Kenichi Morikawa and Tomoko Date for helpful advice. This study was supported by a grant-in-Aid from the Ministry of Health, Labor and Welfare of Japan.

References

Alessi, D.R., 1997. The protein kinase C inhibitors Ro 318220 and GF 109203X are equally potent inhibitors of MAPKAP kinase-1β (Rsk-2) and p70 S6 kinase. FEBS Lett. 402, 121–123.

Date, T., Kato, T., Miyamoto, M., Zhao, Z., Yasui, K., Mizokami, M., Wakita, T., 2004. Genotype 2a hepatitis C virus subgenomic replicon can replicate in HepG2 and IMY-N9 cells. J. Biol. Chem. 279, 22371–22376.

Fukazawa, H., Mizuno, S., Uehara, Y., 1995. A microplate assay for quantitation of anchorage-independent growth of transformed cells. Anal. Biochem. 228, 83–90.

Gekeler, V., Boer, R., Ise, W., Sanders, K.H., Schächtele, C., Beck, J., 1995. The specific bisindolylmaleimide PKC-inhibitor GF 109203X efficiently modulates MRP-associated multiple drug resistance. Biochem. Biophys. Res. Commun. 206, 119–126.

Ishida, H., Li, K., Yi, M., Lemon, S.M., 2007. p21-activated kinase 1 is activated through the mammalian target of rapamycin/p70 S6 kinase pathway and regulates the replication of hepatitis C virus in human hepatoma cells. J. Biol. Chem. 282, 11836–11848.

James, D., 1999. A simple and reliable protocol for the detection of apple stem grooving virus by RT-PCR and in a multiplex PCR assay. J. Virol. Methods 83, 1–9.

Kato, T., Date, T., Miyamoto, M., Furusaka, A., Tokushige, K., Mizokami, M., Wakita, T., 2003. Efficient replication of the genotype 2a hepatitis C virus subgenomic replicon. Gastroenterology 125, 1808–1817.

Lohmann, V., Körner, F., Koch, J., Herian, U., Theilmann, L., Bartenschlager, R., 1999. Replication of subgenomic hepatitis C virus RNAs in a hepatoma cell line. Science 285, 110–113.

Marmy-Conus, N., Hannan, K.M., Pearson, R.B., 2002. Ro 31-6045, the inactive analogue of the protein kinase C inhibitor Ro 31-8220, blocks in vivo activation of p70(s6k)/p85(s6k): implications for the analysis of S6K signalling. FEBS Lett. 519, 135–140.

Merritt, J.E., Sullivan, J.A., Drew, L., Khan, A., Wilson, K., Mulqueen, M., Harris, W., Bradshaw, D., Hill, C.H., Rumsby, M., Warr, R., 1999. The bisindolylmaleimide protein kinase C inhibitor, Ro 32-2241, reverses multidrug resistance in KB tumour cells. Cancer Chemother. Pharmacol. 43, 371–378.

Roberts, N.A., Haworth, R.S., Avkiran, M., 2005. Effects of bisindolylmaleimide PKC inhibitors on p90RSK activity in vitro and in adult ventricular myocytes. Br. J. Pharmacol. 145, 477–489.

Robey, R.W., Shukla, S., Steadman, K., Obrzut, T., Finley, E.M., Ambudkar, S.V., Bates, S.E., 2007. Inhibition of ABCG2-mediated transport by protein kinase inhibitors with a bisindolylmaleimide or indolocarbazole structure. Mol. Cancer Ther. 6, 1877–1885.

Rowhani, A., Maningas, M.A., Lile, L.S., Daubert, S.D., Golino, D.A., 1995. Development of a detection system for viruses of woody plants based on analysis of immobilized virions. Phytopathology 85, 347–352.

Suehiro, N., Matsuda, K., Okuda, S., Natsuaki, T., 2005. A simplified method for obtaining plant viral RNA for RT-PCR. J. Virol. Methods 125, 67–73.

Suzuki, T., Omata, K., Satoh, T., Miyasaka, T., Arai, C., Maeda, M., Matsuno, T., Miyamura, T., 2005. Quantitative detection of hepatitis C virus (HCV) RNA in saliva and gingival crevicular fluid of HCV-infected patients. J. Clin. Microbiol. 43, 4413–4417.

Takeuchi, T., Katsume, A., Tanaka, T., Abe, A., Inoue, K., Tsukiyama-Kohara, K., Kawaguchi, R., Tanaka, S., Kohara, M., 1999. Real-time detection system for quantification of hepatitis C virus genome. Gastroenterology 116, 636–642.

Toullec, D., Pianetti, P., Coste, H., Bellevergue, P., Grand-Perret, T., Ajakane, M., Baudet, V., Boissin, P., Boursier, E., Loriolle, F., Duhamel, L., Charon, D., Kirilovsky, J., 1991. The bisindolylmaleimide GF 109203X is a potent and selective inhibitor of protein kinase C. J. Biol. Chem. 266, 15771–15781.

Wakita, T., Pietschmann, T., Kato, T., Date, T., Miyamoto, M., Zhao, Z., Murthy, K., Habermann, A., Kräusslich, H., Mizokami, M., Bartenschlager, R., Liang, T.J., 2005. Production of infectious hepatitis C virus in tissue culture from a cloned viral genome. Nat. Med. 11, 791–796.

Zhang, Y., Weady, P., Duggal, R., Hao, W., 2008. Novel chimeric genotype 1b/2a hepatitis C virus suitable for high-throughput screening. Antimicrob. Agents Chemother. 52, 666–674.

Zhu, G., Conner, S., Zhou, X., Shih, C., Brooks, H.B., Considine, E., Dempsey, J.A., Ogg, C., Patel, B., Schultz, R.M., Spencer, C.D., Teicher, B., Watkins, S.A., 2003. Synthesis of quinolinyl/isoquinolinyl [a] pyrrolo [3,4-c] carbazoles as cyclin D1/CDK4 inhibitors. Bioorg. Med. Chem. Lett. 13, 1231–1235.

doi:10.1016/j.jmb.2009.04.057 J. Mol. Biol. (2009) 390, 221–230

JMB

Available online at www.sciencedirect.com

ScienceDirect

ELSEVIER

Activities of Various FLP Recombinases Expressed by Adenovirus Vectors in Mammalian Cells

Saki Kondo[1], Yuki Takata[1,3], Masakazu Nakano[1,2], Izumu Saito[1] and Yumi Kanegae[1]*

[1]*Laboratory of Molecular Genetics, Institute of Medical Science, University of Tokyo, 4-6-1 Shirokanedai, Minato-ku, Tokyo 108-8639, Japan*

[2]*Department of Genomic Medical Sciences, Kyoto Prefectural University of Medicine, Kawaramachi-Hirokoji Kamigyo-ku, Kyoto 602-8566, Japan*

[3]*Manufacturing Technology Kokando Co.,Ltd, 2-9-1 Umezawacho,Toyama 930-0055, Japan*

Received 19 December 2008; received in revised form 24 April 2009; accepted 27 April 2009
Available online 3 May 2009

Edited by B. Connolly

FLP, like Cre, is a frequently employed site-specific recombinase. Because wild-type FLP (wtFLP) is thermolabile, a thermostable FLP mutant (FLPe) has been developed for efficient recombination of FLP in studies using mammalian cells and animals. FLPe and wtFLP have been compared in multiple assays *in vitro* and *in vivo*, and in mouse genetics, FLPe has been shown to be very effective like Cre. Here we show an adenovirus vector (AdV) system to be valuable for quantitative measurements of the enzyme activity in mammalian cells and, using this system, precisely compare activities of wtFLP and FLPe. Unexpectedly, we found that the recombination efficiency of FLPe enzyme was lower on a molar basis than that of wtFLP even at 37 °C and, consequently, that the higher recombination yield per transduced AdV genome expressing FLPe compared to wtFLP was due not to inherently higher enzyme activity, but rather to higher steady-state levels of FLPe by its thermostability. Therefore, trying to increase FLPe levels further, we generated a "humanized" FLPe (hFLPe) gene with codon usage optimized for mammals. hFLPe produced about 10-fold more FLPe enzyme in transfection experiments than FLPe, as expected. However, hFLPe-expressing AdV was unstable and could not be prepared without deletion, suggesting that a subtle deleterious effect of FLP on 293 cells may exist. With hFLPe-expressing AdV thus unavailable, of the AdV constructs tested, AdV-expressing FLPe yielded the most recombined targets, despite the lower recombination efficiency of FLPe per enzyme molecule compared with that of wtFLP. We found hFLPe to be valuable for plasmid transfection, and its properties are probably suitable for experiments involving cell lines and transgenic mice.

Keywords: FLP; FLPe; recombinase; adenovirus vector; mammalian cell

Introduction

Site-specific recombinases for analyzing gene function are an important tool for both *in vitro* and *in vivo* studies. Recombinases can induce a deletion, insertion, or inversion of DNA sequences by connecting their target sequences without requiring any other specific factor; these DNA rearrangements can mediate gene activation and inactivation. FLP recombinase, derived from *Saccharomyces cerevisiae*, is a member of the λ integrase family and recognizes a 34-base-pair (bp) FRT (FLP recognition site) recognition target sequence; by now well characterized, FLP has been utilized for gene regulation in plants,[1,2] *Drosophila*,[3,4] mammalian cell cultures,[5–7] and mouse transgenics.[8–10] Another site-specific recombinase, Cre[11–14] (derived from bacteriophage P1), is used similarly; however, Cre has been reported to be toxic to cells not only during constitutive expression,[15–17] but also during transient expression.[18] Therefore, the use of Cre is sometimes problematic. In contrast, FLP has never been reported to be toxic.

While Cre activity is stable at temperatures over 37 °C,[19] the optimum temperature of wild-type FLP (wtFLP) is about 30 °C due to its poor thermostability.[19] The drawback was overcome by the development of a thermostable mutant of FLP

*Corresponding author. E-mail address: kanegae@ims.u-tokyo.ac.jp.

Abbreviations used: wt, wild type; wtFLP, wild-type FLP; FLPe, thermostable FLP mutant; AdV, adenovirus vector; hFLPe, humanized FLPe; FRT, FLP recognition site; ES, embryonic stem; GFP, green fluorescent protein; pA, polyadenylation; FACS, fluorescence-activated cell sorter; MOI, multiplicity of infection.